Department of Energy
Carlsbad Field Office
P. O. Box 3090
Carlsbad, New Mexico 88221

MAY 25 2016

Mr. Jonathan D. Edwards, Director
Radiation Protection Division
U.S. Environmental Protection Agency
1200 Pennsylvania Ave, NW - MC 6608T
Washington, D.C. 20460

Subject: Response to the U.S. Environmental Protection Agency Letters Dated June 5, 2015, July 30, 2015, and February 26, 2016, Regarding the 2014 Compliance Recertification Application

Dear Mr. Edwards:

The U.S. Department of Energy (DOE) Carlsbad Field Office (CBFO) is providing responses to seven of the U.S. Environmental Protection Agency (EPA) completeness questions on the 2014 Compliance Recertification Application from the EPA letters dated June 5, 2015, and July 30, 2015, and addendums to three of the DOE/CBFO responses previously submitted to the EPA. Two addendums to the original DOE/CBFO response to 1-23-12, *WIPP-Specific Organic Complexation Data* and 2-C-6, *MgO Hydration Rate* are being submitted based on an agreement made at a DOE/CBFO and EPA technical exchange meeting in Albuquerque, New Mexico held February 2 and 3, 2016. One addendum to the original DOE/CBFO response to 2-C-4, *Hydromagnesite Conversion Rate* is being submitted as requested in the EPA's February 26, 2016, letter that clarified its original completeness question.

With this submittal, the DOE/CBFO is providing responses to all of the remaining EPA completeness questions on the 2014 Compliance Recertification Application received to date. This submittal includes four enclosures:

- Enclosure 1 is a hard copy of the EPA's comments and the DOE/CBFO responses and addendums;
- Enclosure 2 (on disc) provides the electronic version of the references as noted in each response. Copyrighted references, marked with an asterisk in "References" of Enclosure 1, are not provided in enclosure 2. If there are specific copyrighted references the EPA needs, the DOE/CBFO will work to obtain a copy;
- Enclosure 3 is the "Status Report of DOE Responses to EPA Completeness Questions." The Table shows the status of responses to the EPA comments received on December 17, 2014, February 27, 2015, June 5, 2015, July 30, 2015, and February 26, 2016;
- Enclosure 4 is the "CRA-2014 Errata Tracking." The table is a cumulative list of errata that have been identified and corrected.

If you have any questions regarding this response, please contact Russ Patterson at (575) 234-7457.

Sincerely,

Todd Shrader, Manager
Carlsbad Field Office

Enclosures (4)

CBFO:EPD:RP:MR:16-0534:UFC 5486.00

cc: w/enclosures

F. Marcinowski, DOE/HQ	*ED
D. Tonkay, DOE/HQ	ED
A. Harris, DOE/HQ	ED
C. Gadbury, DOE/CBFO	ED
W. Mouser, DOE/CBFO	ED
G. Basabilvazo, DOE/CBFO	ED
R. Patterson, DOE/CBFO	ED
A. Ward, DOE/CBFO	ED
T. Peake, EPA/ORIA	ED
K. Economy, EPA/ORIA	ED
J. Walsh, EPA/ORIA	ED
S. Ghose, EPA/ORIA	ED
R. Lee, EPA/ORIA	ED
N. Stone, EPA Region 6	ED
CBFO M&RC	

*ED denotes electronic distribution

EPA Comment

3-C-3. Adequacy of EQ3/6 Database. *The actinide solubility and aqueous speciation data in the EQ3/6 database DATA0.FM1 was last updated using data available in 2002 (Giambalvo 2003, Nowak 2005). Since 2002, relevant data have been developed in investigations carried out by WIPP investigators and by outside researchers. The absence of an update to the EQ3/6 database despite more than a decade of potentially relevant new data leads to the following observations:*

- *In CRA-2014 Appendix SOTERM Sections 3.3 and 3.7, DOE reviewed the chemistry of thorium and americium, respectively, including data that has become available since the last EQ3/6 database update. However, these data (such and Neck et al. 2002, Neck et al. 2003, Altmaier et al. 2004, Altmaier et al. 2005, Altmaier et al. 2006, Borkowski et al. 2012, Neck et al. 2009) were not used to revise the EQ3/6 database.*
- *Xiong (2011) experimentally determined the solubilities of natural and synthetic hydromagnesite samples and calculated a different solubility for synthetic hydromagnesite than the solubility in the EQ3/6 database. An assessment was not provided in the CRA of the possible effects of this different solubility on CO_2 fugacities, calculated pH values and actinide solubilities in WIPP repository brines.*
- *Borkowski et al. (2010) determined the stability constant for the neodymium-tetraborate aqueous species and also calculated Pitzer ion-interaction parameters. These data were not incorporated into the EQ3/6 database, even though WIPP brines contain borate, boric acid or hydroxyl polynuclear species and complexation of the +III actinides by tetraborate could increase solubilities modeled for PA.*
- *Thakur et al. (2014) determined a β^0_{101} for $AmEDTA^-$ (20.55) that differs from the value in DATA0.FM1 (18.97). Because $AmEDTA^-$ is the predominant Am(III) aqueous species in WIPP brines, the β^0_{101} for $AmEDTA^-$ could significantly affect aqueous Am speciation and solubilities, but the revised value was not included in the EQ3/6 database.*

DOE maintained at the time of the CRA-2009 PABC that the effects of not updating the EQ3/6 database with new data available at that time were conservative, because higher actinide solubilities would be predicted using the unrevised database. However, the cumulative effects of the new data that are now available may be non-conservative and must be quantitatively evaluated. DOE must: 1) carry out and document a thorough review of all available +III and +IV actinide aqueous speciation and solubility data and hydromagnesite solubility data; 2) use the results of this review to defensibly update the EQ3/6 database; and 3) use this revised database to recalculate the actinide solubilities and associated uncertainty distributions for PA. DOE must provide the documentation of these components as part of the CRA.

Altmaier, M., V. Neck and T. Fanghänel. 2004. Solubility and colloid formation of Th(IV) in concentrated NaCL and $MgCl_2$ solution. Radiochimica Acta 92:537-543.

Altmaier, M., V. Neck, M.A. Denecke, R. Yin and T. Fanghänel. 2006. Solubility of $ThO_2 \cdot xH_2O$(am) and the formation of ternary Th(IV) hydroxide-complexes in $NAHCO_3$-Na_2CO_3 solutions containing 0-4 M NaCL. Radiochimica Acta 94:495-500.

Altmaier, M., V. Neck, R. Müller and T. Fanghänel. 2005. Solubility of $ThO_2 \cdot xH_2O$(am) in carbonate solution and the formation of ternary Th(IV) hydroxide-carbonate complexes. Radiochimica Acta 93:83-92.

Borkowski, M., M. Richmann, D.T. Reed and Y. Xiong. 2010. Complexation of Nd(III) with tetraborate ion and its effect on actinide(III) solubility in WIPP brine. Radiochimica Acta 98:577-582.

Borkowski, M., M. Richmann and J.F. Lucchini. 2012. Solubility of An(IV) in WIPP brine: thorium analog studies in WIPP simulated brine. Los Alamos National Laboratory LCO-ACP-17.

Giambalvo, E.R. 2003. Release of FMT Database FMT_021120.CHEMDAT. Memorandum to L.H. Brush, March 10, 2003, ERMS 526372.

Neck, V., M. Altmaier, R. Müller, A. Bauer, T. Fanghänel and J.I. Kim. 2003. Solubility of crystalline thorium dioxide. Radiochimica Acta 91:253-262.

Neck, V. M. Altmaier, T. Rabung, J. Lützenkirchen and T. Fanghänel. 2009. Thermodynamics of trivalent actinides and neodymium in NaCl, $MgCl_2$, and $CaCl_2$ solutions: solubility, hydrolysis, and ternary Ca-M(III)-OH complexes. Pure and Applied Chemistry 81:1555-1568.

Neck, V., R. Müller, M. Bouby, M. Altmaier, J. Rothe, M.A. Denecke, and J.I. Kim. 2002. Solubility of Amorphous Th(IV) Hydroxide-Application of LIBD to Determine the Solubility Product and EXAFS for Aqueous Speciation. Radiochimica Acta 90:485-494.

Nowak, E.J. 2005. Recommended Change in the FMT Thermodynamic Data Base. Memorandum to L.H. Brush, April 1, Sandia National Laboratories, Carlsbad, New Mexico, ERMS 539227.

Thakur, P., Y. Xiong, M. Borkowski and G.R. Choppin. 2014. Improved thermodynamic model for interaction of EDTA with trivalent actinides and lanthanide to ionic strength of 6.60 m. Geochimica et Cosmochimica Acta 133:299-312.

Xiong, Y. 2011. Experimental determination of solubility constant of hydromagnesite (5424) in NaCl solutions up to 4.4 m at room temperature. Chemical Geology 284:262-269.

DOE Response

The EPA is correct in noting that the actinide solubility and aqueous speciation data in the EQ3/6 database DATA0.FM1 was last updated using data available in 2002 (Giambalvo 2003; Nowak 2005). However, it is worth noting that the database had a minor update after 2002 regarding non-actinide species with the addition of whewellite, $CaC_2O_4 \cdot H_2O$, and phase 5, $Mg_3Cl(OH)_5 \cdot 4H_2O$ (Xiong 2004, 2005, 2009; Xiong et al. 2009, 2010). To be clear, the reactions shown in Attachment A of this response, Tables 1 through 7, constitute the WIPP model for near-field geochemistry that was used for CRA-2004, CRA-2009, associated PABCs, and CRA-2014. The EQ3/6 database DATA0.FM1 (Xiong 2011) contains the thermodynamic constants (equilibrium constants) for the reactions and the Pitzer parameter values for the species shown in reactions without yellow highlight in Tables 1 through 7 of Attachment A.

The EPA is also correct in noting that WIPP-relevant data have been developed since 2002 in investigations carried out by WIPP investigators and by outside researchers. Consequently, the DOE has updated the EQ3/6 database and created DATA0.FM2 (Domski 2015; Xiong and Domski 2016). Chemical reactions with a yellow highlight in Tables 2, 3, 4, and 7, and the reactions for lead species in Table 8 of Attachment A have been added to the latest EQ3/6 database, DATA0.FM2. This set of comprehensive lead parameters significantly improves our understanding of the near-field geochemistry because there are sizable inventories of lead in both the waste and shielding (Bryson 2015). Documentation of how DATA0.FM2 was created is provided in the analysis report entitled, *Updating the WIPP Thermodynamic Database*, by Xiong and Domski (2016).

Prompted by EPA comments 3-C-3, 3-C-4, and 3-C-5, DOE compiled this analysis report (Xiong and Domski 2016) in order to provide detailed background information in support of the responses. The DOE response to 3-C-3 is best reviewed alongside the analysis report.

The EPA's specific comments on 3-C-3 are shown in italics below, immediately followed by the DOE response. EPA wrote first,

> *In CRA-2014 Appendix SOTERM Sections 3.3 and 3.7, DOE reviewed the chemistry of thorium and americium, respectively, including data that has become available since the last EQ3/6 database update. However, these data (such as Neck et al. 2002, Neck et al. 2003, Altmaier et al. 2004, Altmaier et al. 2005, Altmaier et al. 2006, Borkowski et al. 2012, Neck et al. 2009) were not used to revise the EQ3/6 database.*

Please see Section 3.II and Appendices A and B of Xiong and Domski (2016) (ERMS 565730) for a technical discussion of why these specific thorium and americium data were not included in the revised EQ3/6 database (i.e., DATA0.FM2).

EPA also noted,

> *Xiong (2011) experimentally determined the solubilities of natural and synthetic hydromagnesite samples and calculated a different solubility for synthetic hydromagnesite than the solubility in the EQ3/6 database. An assessment was not provided in the CRA of the possible effects of this different solubility on CO2 fugacities, calculated pH values and actinide solubilities in WIPP repository brines.*

Please see Section 3.I.(A) of Xiong and Domski (2016) for a technical assessment of the impact of natural versus synthetic hydromagnesite on f_{CO_2}, which influences americium solubility. Baseline solubility calculations (Domski and Xiong 2015) performed using DATA0.FM2 indicate that the resulting fugacity of CO_2 (f_{CO_2}) decreased from 3.14×10^{-6} atm (the value predicted using DATA0.FM1) to 5.84×10^{-7} atm (the value predicted using DATA0.FM2). The pcH (negative log hydrogen ion concentration on a molar scale) in GWB changed from 9.5 (the value predicted using DATA0.FM1) to 9.6 (the value predicted using DATA0.FM2). The pcH in ERDA-6 changed from 9.0 (the value predicted using DATA0.FM1) to 9.2 (the value predicted using DATA0.FM2).

EPA stated further,

> *Borkowski et al. (2010) determined the stability constant for the neodymium-tetraborate aqueous species and also calculated Pitzer ion-interaction parameters. These data were not incorporated into the EQ3/6 database, even though WIPP brines contain borate, boric acid or hydroxyl polynuclear species and complexation of the +III actinides by tetraborate could increase solubilities modeled for PA.*

Please see Sections 3.I.(D) and 3.I.(E) of Xiong and Domski (2016) (ERMS 565730) for a technical discussion of why the calculations contained in Borkowski et al. (2010) to determine the stability constant for the neodymium-tetraborate aqueous species and Pitzer ion-interaction parameters were not included in the revised EQ3/6 database.

EPA wrote,

> *Thakur et al. (2014) determined a β^0_{101} for AmEDTA- (20.55) that differs from the value in DATA0.FM1 (18.97). Because AmEDTA- is the predominant Am(III) aqueous species in WIPP brines, the β^0_{101} for AmEDTA- could significantly affect aqueous Am speciation and solubilities, but the revised value was not included in the EQ3/6 database.*

Please see Sections 3.I.(B) and 3.I.(C) of Xiong and Domski (2016) for a technical discussion of the approach to incorporating AmEDTA- into the revised EQ3/6 database.

EPA finally mentioned,

> *DOE maintained at the time of the CRA-2009 PABC that the effects of not updating the EQ3/6 database with new data available at that time were conservative, because higher actinide solubilities would be predicted using the unrevised database. However, the cumulative effects of the new data that are now available may be non-conservative and must be quantitatively evaluated. DOE must: 1) carry out and document a thorough review of all available +III and +IV actinide aqueous speciation and solubility data and hydromagnesite solubility data; 2) use the results of this review to defensibly update the EQ3/6 database; and 3) use this revised database to recalculate the actinide solubilities and associated uncertainty distributions for PA. DOE must provide the documentation of these components as part of the CRA.*

The thorough review of all available +III and +IV actinide aqueous speciation and solubility data can be found in Appendices A and B of Xiong and Domski (2016). The methodology used to revise the EQ3/6 database is described in Section 3, Subsection 2, of Xiong and Domski (2016). The recalculated actinide solubilities and associated uncertainty distributions using the revised EQ3/6 database are documented in Domski and Xiong (2015) and Xiong and Domski (2015), respectively.

References:

Bryson, D. 2015. Letter to Mr. Jonathan D. Edwards, Director, Radiation Protection Division (Subject: Response to the U.S. Environmental Protection Agency Letters Dated February 27, 2015 and June 5, 2015 Regarding the 2014 Compliance Recertification Application). September 25, 2015. Carlsbad Field Office, Carlsbad, NM.

Domski, P.S. 2015. Memo AP-173, EQ3/6 Database Update: DATA0.FM2. Memorandum to WIPP Records, October 27, 2015. ERMS 564914. Sandia National Laboratories, Carlsbad, NM.

Domski, P., and Y.-L. Xiong. 2015. Prediction of Baseline Actinide Solubilities with an Updated EQ3/6 Thermodynamic Database (DATA0.FM2) in Response to EPA Completeness Comment 3-C-3 for CRA 2014. ERMS 565032. Sandia National Laboratories, Carlsbad, NM.

Giambalvo, E.R. 2003. Memorandum to L.H. Brush (Subject: Release of FMT Database FMT_021120.CHEMDAT). March 10, 2003. ERMS 526372. Sandia National Laboratories, Carlsbad, NM.

Nowak, E.J. 2005. Memorandum to L.H. Brush (Subject: Recommended Change in the FMT Thermodynamic Data Base). ERMS 539227. Sandia National Laboratories, Carlsbad, NM.

Xiong, Y.-L. 2004. A Correction of the Molecular Weight of Oxalate in FMT_021120.CHEMDAT, and Incorporation of Calcium Oxalate Monohydrate (Whewellite) into CHEMDAT with Its Recommended Dimensionless Standard Chemical Potential Value. ERMS 535813. Sandia National Laboratories, Carlsbad, NM.

Xiong, Y.-L. 2005. Release of FMT_050405.CHEMDAT. ERMS 539304. Sandia National Laboratories, Carlsbad, NM.

Xiong, Y-L. 2009. Release of FMT_090720.CHEMDAT. ERMS 551706. Sandia National Laboratories, Carlsbad, NM.

Xiong, Y.-L. 2011. Email to J.J. Long (Subject: Release of EQ3/6 Database DATA0.FM1). March 9, 2011. ERMS 555152 and associated document ERMS 555154. Sandia National Laboratories, Carlsbad, NM.

Xiong, Y.-L., and P.S. Domski. 2015. Uncertainty analysis of actinide solubilities for the WIPP CRA-2014 PABC with the updated database. ERMS 565125. Sandia National Laboratories, Carlsbad, NM.

Xiong, Y-L., and P.S. Domski. 2016. Updating the WIPP Thermodynamic Database. Analysis Report for AP-173, Revision 1. ERMS 565730. Sandia National Laboratories, Carlsbad, NM.

Xiong, Y.-L., H.-R. Deng, M. Nemer and S. Johnsen. 2009. Thermodynamic Data for Phase 5 ($Mg_3Cl(OH)_5 \cdot 4H_2O$) Determined from Solubility Experiments. ERMS 551294. Sandia National Laboratories, Carlsbad, NM.

Xiong, Y.-L., H.-R. Deng, M. Nemer and S. Johnsen. 2010. Experimental determination of the solubility constant for magnesium chloride hydroxide hydrate ($Mg_3Cl(OH)_5 \cdot 4H_2O$, phase 5) at room temperature, and its importance to nuclear waste isolation in geological repositories in salt formations. Geochimica et Cosmochimica Acta 74:4605-4611.*

* Copyrighted reference not provided in Enclosure 2.

ATTACHMENT A

REACTIONS IN THE EQ3/6 DATABASES DATA0.FM1 AND DATA0.FM2

Table 1. Reactions for Major Ions and Minerals Included in DATA0.FM1 and DATA0.FM2

(I-1) $H_2O = OH^- + H^+$

(I-2) $Ca^{2+} + 2H_2O = Ca(OH)_2(portlandite) + 2H^+$

(I-3) $Na^+ + Cl^- = NaCl(halite)$

(I-4) $K^+ + Cl^- = KCl(sylvite)$

(I-5) $Ca^{2+} + 2Cl^- + 4H_2O = CaCl_2 \cdot 4H_2O(cr)$

(I-6) $4Ca^{2+} + 2Cl^- + 19H_2O = Ca_4Cl_2(OH)_6 \cdot 13H_2O(CaOxychloride\_A) + 6H^+$

(I-7) $2Ca^{2+} + 2Cl^- + 3H_2O = Ca_2Cl_2(OH)_2 \cdot H_2O(CaOxychloride\_B) + 2H^+$

(I-8) $K^+ + Mg^{2+} + 3Cl^- + 6H_2O = KMgCl_3 \cdot 6H_2O(carnallite)$

(I-9) $H^+ + HCO_3^- = CO_2(aq) + H_2O$

(I-10) $HCO_3^- = CO_3^{2-} + H^+$

(I-11) $Na^+ + HCO_3^- = NaHCO_3(nahcolite)$

(I-12) $3Na^+ + 2HCO_3^- + 2H_2O = Na_3H(CO_3)_2 \cdot 2H_2O(trona) + H^+$

(I-13) $2Na^+ + HCO_3^- + 10H_2O = Na_2CO_3 \cdot 10H_2O(natron) + H^+$

(I-14) $2Na^+ + HCO_3^- + 7H_2O = Na_2CO_3 \cdot 7H_2O(cr) + H^+$

(I-15) $2Na^+ + HCO_3^- + H_2O = Na_2CO_3 \cdot H_2O(thermonatrite) + H^+$

(I-16) $K^+ + HCO_3^- = KHCO_3(kalicinite)$

(I-17) $2K^+ + HCO_3^- + 1.5H_2O = K_2CO_3 \cdot 3/2H_2O(cr) + H^+$

(I-18) $8K^+ + 6HCO_3^- + 3H_2O = K_8H_4(CO_3)_6 \cdot 3H_2O(cr) + 2H^+$

(I-19) $K^+ + Na^+ + HCO_3^- + 6H_2O = KNaCO_3 \cdot 6H_2O(cr) + H^+$

(I-20) $2K^+ + Na^+ + 2HCO_3^- + 2H_2O = K_2NaH(CO_3)_2 \cdot 2H_2O(K\text{-}trona) + H^+$

(I-21) $Ca^{2+} + HCO_3^- = CaCO_3(aragonite) + H^+$

(I-22) $Ca^{2+} + HCO_3^- = CaCO_3(calcite) + H^+$

(I-23) $Ca^{2+} + 2Na^+ + 2HCO_3^- + 5H_2O = CaNa_2(CO_3)_2 \cdot 5H_2O(gaylussite) + 2H^+$

(I-24) $2Na^+ + Ca^{2+} + 2HCO_3^- + 2H_2O = Na_2Ca(CO_3)_2 \cdot 2H_2O(pirssonite) + 2H^+$

(I-25) $SO_4^{2-} + H^+ = HSO_4^- + H^+$

(I-26) $Ca^{2+} + SO_4^{2-} = CaSO_4(anhydrite)$

(I-27) $Ca^{2+} + SO_4^{2-} + 2H_2O = CaSO_4 \cdot 2H_2O(gypsum)$

(I-28) $2K^+ + SO_4^{2-} = K_2SO_4(arcanite)$

(I-29) $8K^+ + 6H^+ + 7SO_4^{2-} = K_8H_6(SO_4)_7(misenite)$

(I-30) $3K^+ + H^+ + 2SO_4^{2-} = K_3H(SO_4)_2(cr)$

(I-31) $K^+ + Ca^{2+} + 2SO_4^{2-} + H_2O = K_2Ca(SO_4)_2 \cdot H_2O(syngenite)$

(I-32) $2Na^+ + SO_4^{2-} + 10H_2O = Na_2SO_4 \cdot 10H_2O(mirabilite)$

(I-33) $2Na^+ + SO_4^{2-} = Na_2SO_4(thenardite)$

(I-34) $Na^+ + H^+ + 2SO_4^{2-} = Na_3H(SO_4)_2(cr)$

(I-35) $Na^+ + 3K^+ + 2SO_4^{2-} = NaK_3(SO_4)_2(aphthitalite, galerite)$

(I-36) $2Na^+ + Ca^{2+} + 2SO_4^{2-} = Na_2Ca(SO_4)_2(glauberite)$

(I-37) $4Na^+ + Ca^{2+} + 3SO_4^{2-} + 2H_2O = Na_4Ca(SO_4)_3 \cdot 2H_2O(labile\ salt)$

(I-38) $HPO_4^{2-} + 2H^+ = H_3PO_4(aq)$

(I-39) $HPO_4^{2-} + H^+ = H_2PO_4^- + H^+$

(I-40) $HPO_4^{2-} = PO_4^{3-} + H$

1

Table 2. Reactions for Mg-bearing Species (Related to MgO) Included in DATA0.FM1 and DATA0.FM2

(II-1)	$Mg^{2+} + H_2O = MgOH^+ + H^+$
(II-2)	$Mg^{2+} + 2H_2O = Mg(OH)_2(brucite) + 2H^+$
(II-3)	$Mg^{2+} + 2Cl^- + 6H_2O = MgCl_2 \cdot 6H_2O(bischofite)$
(II-4)	$2Mg^{2+} + Cl^- + 7H_2O = Mg_2Cl(OH)_3 \cdot 4H_2O(phase\ 3) + 3H^+$
(II-5)	$3Mg^{2+} + Cl^- + 9H_2O = Mg_3Cl(OH)_5 \cdot 4H_2O(phase\ 5) + 5H^+$
(II-6)	$2Mg^{2+} + Ca^{2+} + 6Cl^- + 12H_2O = Mg_2CaCl_6 \cdot 12H_2O(tachyhydrite)$
(II-7)	$K^+ + Mg^{2+} + 3Cl^- + 6H_2O = KMgCl_3 \cdot 6H_2O(carnallite)$
(II-8)	$Mg^{2+} + HCO_3^- = MgCO_3(magnesite) + H^+$
(II-9)	$Mg^{2+} + HCO_3^- + 3H_2O = MgCO_3 \cdot 3H_2O(nesquehonite) + H^+$
(II-10)	$4Mg^{2+} + 3HCO_3^- + 5H_2O = Mg_4(CO_3)_3(OH)_2 \cdot 3H_2O(hydromagnesite4323) + 5H^+$
(II-11)	$5Mg^{2+} + 4HCO_3^- + 6H_2O = Mg_5(CO_3)_4(OH)_2 \cdot 4H_2O(hydromagnesite5424) + 6H^+$
(II-12)	$2K^+ + Mg^{2+} + 2SO_4^{2-} + 4H_2O = K_2Mg(SO_4)_2 \cdot 4H_2O(leonite)$
(II-14)	$2Na^+ + Mg^{2+} + 2SO_4^{2-} + 2H_2O = Na_2Mg(SO_4)_2 \cdot 4H_2O(boedite)$
(II-15)	$Mg^{2+} + SO_4^{2-} + 7H_2O = MgSO_4 \cdot 7H_2O(epsomite)$
(II-16)	$Mg^{2+} + SO_4^{2-} + 6H_2O = MgSO_4 \cdot 6H_2O(hexahydrite)$
(II-17)	$Mg^{2+} + SO_4^{2-} + H_2O = MgSO_4 \cdot H_2O(kieserite)$
(II-18)	$K^+ + Mg^{2+} + Cl^- + SO_4^{2-} + 3H_2O = KMgClSO_4 \cdot 3H_2O(kainite)$
(II-19)	$Mg^{2+} + SO_4^{2-} = MgSO_4(aq)$ [a]

Note:
[a] The (II-19) reaction was added into DATA0.FM2.

1
2 Table 3. Reactions for Organic Ligands Included in DATA0.FM1 and DATA0.FM2

(III-1) $Mg^{2+} + Acetate^{-} = MgAcetate^{+}$

(III-2) $Ca^{2+} + Acetate^{-} = CaAcetate^{+}$

(III-3) $Citrate^{3-} + 3H^{+} = H_3Citrate\ (aq)$

(III-4) $Citrate^{3-} + 2H^{+} = H_2Citrate^{-}$

(III-5) $Citrate^{3-} + H^{+} = HCitrate^{2-}$

(III-6) $Mg^{2+} + Citrate^{3-} = MgCitrate^{-}$

(III-7) $Ca^{2+} + Citrate^{3-} = CaCitrate^{-}$

(III-8) $Ca_3(Citrate)_2 \cdot 4H_2O\ (earlandite) = 3Ca^{2+} + 2Citrate^{3-} + 4H_2O$ [a]

(III-9) $EDTA^{4-} + 4H^{+} = H_4EDTA(aq)$

(III-10) $EDTA^{4-} + 3H^{+} = H_3EDTA^{-}$

(III-11) $EDTA^{4-} + 2H^{+} = H_2EDTA^{2-}$

(III-12) $EDTA^{4-} + H^{+} = HEDTA^{3-}$

(III-13) $Mg^{2+} + EDTA^{4-} = MgEDTA^{2-}$

(III-14) $Ca^{2+} + EDTA^{4-} = CaEDTA^{2-}$

(III-15) $Ca_2EDTA(s) = 2Ca^{2+} + EDTA^{4-}$ [a]

(III-16) $Oxalate^{2-} + 2H^{+} = H_2Oxalate(aq)$

(III-17) $Oxalate^{2-} + H^{+} = HOxalate^{-}$

(III-18) $Mg^{2+} + Oxalate^{2-} = MgOxalate(aq)$

(III-19) $Ca^{2+} + Oxalate^{2-} = CaOxalate(aq)$

(III-20) $Oxalate^{2-} + 2H^{+} + 2H_2O = H_2Oxalate \cdot 2H_2O$

(III-21) $Na^{+} + H^{+} + Oxalate^{2-} + H_2O = NaHOxalate \cdot H_2O$

(III-22) $2Na^{+} + Oxalate^{2-} = Na_2Oxalate$

(III-23) $Ca^{2+} + Oxalate^{2-} + H_2O = CaOxalate \cdot H_2O$

(III-24) $Lactate^{-} + H^{+} = HLactate(aq)$

(III-25) $Acetate^{-} + H^{+} = HAcetate(aq)$

Note:
[a] The (III-8) and (III-15) reactions were added into DATA0.FM2.

3

Table 4. Reactions for An(III) (Actinides in +III Oxidation State) Included in DATA0.FM1 and DATA0.FM2

(IV-1) $AmCO_3^+ + H^+ = Am^{3+} + HCO_3^-$

(IV-2) $Am(CO_3)_2^- + 2H^+ = Am^{3+} + 2HCO_3^-$

(IV-3) $Am(CO_3)_3^{3-} + 3H^+ = Am^{3+} + 3HCO_3^-$

(IV-4) $Am(CO_3)_4^{5-} + 4H^+ = Am^{3+} + 4HCO_3^-$

(IV-5) $Am(OH)^{2+} + H^+ = Am^{3+} + H_2O$

(IV-6) $Am(OH)_2^+ + 2H^+ = Am^{3+} + 2H_2O$

(IV-7) $Am(OH)_3(aq) + 3H^+ = Am^{3+} + 3H_2O$

(IV-8) $AmCl^{2+} = Am^{3+} + Cl^-$

(IV-9) $AmCl_2^+ = Am^{3+} + 2Cl^-$

(IV-10) $AmSO_4^+ = Am^{3+} + SO_4^{2-}$

(IV-11) $Am(SO_4)_2^- = Am^{3+} + 2SO_4^{2-}$

(IV-12) $AmAcetate^{2+} = Am^{3+} + Acetate^-$

(IV-13) $AmCitrate(aq) = Am^{3+} + Citrate^{3-}$

(IV-14) $AmEDTA^- = Am^{3+} + EDTA^{4-}$

(IV-15) $AmLactate^{2+} = Am^{3+} + Lactate^-$

(IV-16) $AmOxalate^+ = Am^{3+} + Oxalate^{2-}$

(IV-17) $AmOHCO_3(s) + 2H^+ = Am^{3+} + H_2O + HCO_3^-$

(IV-18) $Am(OH)_3(s) + 3H^+ = Am^{3+} + 3H_2O$

(IV-19) $NaAm(CO_3)_2 \cdot 6H_2O(s) + 2H^+ = Na^+ + Am^{3+} + 2HCO_3^- + 6H_2O$

(IV-20) $AmPO_4(cr) + H^+ = Am^{3+} + HPO_4^{2-}$

(IV-21) $AmHB_4O_7^{2+} + 9H_2O = Am^{3+} + 4B(OH)_4^- + 3H^+$ [a]

Note:

[a] The (IV-21) reaction was added into DATA0.FM2.

Table 5. Reactions for An(IV) (Actinides in the +IV Oxidation State) Included in DATA0.FM1 and DATA0.FM2

(V-1) $Th(CO_3)_5^{6-} + 5H^+ = Th^{4+} + 5HCO_3^-$

(V-2) $Th(OH)_3(CO_3)^- + 4H^+ = Th^{4+} + 3H_2O + HCO_3^-$

(V-3) $Th(OH)_4(aq) + 4H^+ = Th^{4+} + 4H_2O$

(V-4) $Th(SO_4)_2(aq) = Th^{4+} + 2SO_4^{2-}$

(V-5) $Th(SO_4)_3^{2-} = Th^{4+} + 3SO_4^{2-}$

(V-6) $ThAcetate^{3+} = Th^{4+} + Acetate^-$

(V-7) $Th(Acetate)_2^{2+} = Th^{4+} + 2Acetate^-$

(V-8) $ThCitrate^+ = Th^{4+} + Citrate^{3-}$

(V-9) $ThEDTA(aq) = Th^{4+} + EDTA^{4-}$

(V-10) $ThLactate^{3+} = Th^{4+} + Lactate^-$

(V-11) $Th(Lactate)_2^{2+} = Th^{4+} + 2Lactate^-$

(V-12) $ThOxalate^{2+} = Th^{4+} + Oxalate^{2-}$

(V-13) $ThO_2(am) + 4H^+ = Th^{4+} + 2H_2O$

(V-14) $Th(SO_4)_2 \cdot 9H_2O(s) = Th^{4+} + 2SO_4^{2-} + 9H_2O$

(V-15) $Th(SO_4)_2 \cdot 8H_2O(s) = Th^{4+} + 2SO_4^{2-} + 8H_2O$

(V-16) $Th(SO_4)_2 \cdot Na_2SO_4 \cdot 6H_2O(s) = Th^{4+} + 3SO_4^{2-} + 2Na^+ + 6H_2O$

(V-17) $Th(SO_4)_2 \cdot K_2SO_4 \cdot 4H_2O(s) = Th^{4+} + 3SO_4^{2-} + 2K^+ + 4H_2O$

(V-18) $Th(SO_4)_2 \cdot 2K_2SO_4 \cdot 2H_2O(s) = Th^{4+} + 4SO_4^{2-} + 4K^+ + 2H_2O$

(V-19) $2[Th(SO_4)_2 \cdot 7/2K_2SO_4(s)] = 2Th^{4+} + 11SO_4^{2-} + 14K^+$

Table 6. Reactions for An(V) (Actinides in the +V Oxidation State) Included in DATA0.FM1 and DATA0.FM2

(VI-1)	$NpO_2CO_3^- + H^+ = NpO_2^+ + HCO_3^-$
(VI-2)	$NpO_2(CO_3)_2^{3-} + 2H^+ = NpO_2^+ + 2HCO_3^-$
(VI-3)	$NpO_2(CO_3)_3^{5-} + 3H^+ = NpO_2^+ + 3HCO_3^-$
(VI-4)	$NpO_2(OH)(aq) + H^+ = NpO_2^+ + H_2O$
(VI-5)	$NpO_2(OH)_2^- + 2H^+ = NpO_2^+ + 2H_2O$
(VI-6)	$NpO_2Acetate(aq) = NpO_2^+ + Acetate^-$
(VI-7)	$NpO_2Citrate^{2-} = NpO_2^+ + Citrate^{3-}$
(VI-8)	$NpO_2H_2EDTA^- = NpO_2^+ + EDTA^{4-} + 2H^+$
(VI-9)	$NpO_2HEDTA^{2-} = NpO_2^+ + EDTA^{4-} + H^+$
(VI-10)	$NpO_2EDTA^{3-} = NpO_2^+ + EDTA^{4-}$
(VI-11)	$NpO_2Lactate(aq) = NpO_2^+ + Lactate^-$
(VI-12)	$NpO_2Oxalate^- = NpO_2^+ + Oxalate^{2-}$
(VI-13)	$NpO_2OH(aged) + H^+ = NpO_2^+ + H_2O$
(VI-14)	$NpO_2OH(am) + H^+ = NpO_2^+ + H_2O$
(VI-15)	$2[NaNpO_2CO_3 \cdot 7/2H_2O](s) + 2H^+ = 2NpO_2^+ + 2HCO_3^- + 2Na^+ + 7H_2O$
(VI-16)	$Na_3NpO_2(CO_3)_2(s) + 2H^+ = NpO_2^+ + 2HCO_3^- + 3Na^+$
(VI-17)	$KNpO_2CO_3(s) + H^+ = NpO_2^+ + HCO_3^- + K^+$
(VI-18)	$K_3NpO_2(CO_3)_2(s) + 2H^+ = NpO_2^+ + 2HCO_3^- + 3K^+$

1 Table 7. Reactions for Borate Species Included in DATA0.FM1 and DATA0.FM2

(VII-1)	$B(OH)_4^- + H^+ = B(OH)_3(aq) + H_2O$
(VII-2)	$CaB(OH)_4^+ = Ca^{2+} + B(OH)_4^-$
(VII-3)	$MgB(OH)_4^+ = Mg^{2+} + B(OH)_4^-$
(VII-4)	$B_3O_3(OH)_4^- + 5H_2O = 3B(OH)_4^- + 2H^+$
(VII-5)	$B_4O_5(OH)_4^{2-} + 7H_2O = 4B(OH)_4^- + 2H^+$
(VII-6)	$NaB(OH)_4(aq) = Na^+ + B(OH)_4^-$ [a]
(VII-7)	$Na_2B_4O_7 \cdot 10H_2O$(Na-tetraborate) $= 2Na^+ + 4B(OH)_4^- + 2H^+ + H_2O$
(VII-8)	$B(OH)_3(cr) + H_2O = B(OH)_4^- + H^+$
(VII-9)	$KB_5O_8 \cdot 4H_2O$(K-pentaborate) $+ 8H_2O = K^+ + 5B(OH)_4^- + 4H^+$
(VII-10)	$K_2B_4O_7 \cdot 4H_2O$(K-tetraborate) $+ 5H_2O = 2K^+ + 4B(OH)_4^- + 2H^+$
(VII-11)	$NaBO_2 \cdot 4H_2O$(Na-metaborate) $= Na^+ + B(OH)_4^- + 2H_2O$
(VII-12)	$NaB_5O_8 \cdot 5H_2O$(Na-pentaborate) $+ 7H_2O = Na^+ + 5B(OH)_4^- + 4H^+$
(VII-13)	$NaBO_2 \cdot NaCl \cdot 2H_2O$(teepleite) $= 2Na^+ + B(OH)_4^- + Cl^-$

Note:
[a] The (VII-6) reaction was added into DATA0.FM2.

2

Table 8. Reactions for Pb Species Included in DATA0.FM2

(VIII-1) $Pb^{2+} + Cl^- = PbCl^+$

(VIII-2) $Pb^{2+} + 2Cl^- = PbCl_2(aq)$

(VIII-3) $Pb^{2+} + 3Cl^- = PbCl_3^-$

(VIII-4) $Pb^{2+} + Oxalate^{2-} = PbOxalate(aq)$

(VIII-5) $Pb^{2+} + 2Oxalate^{2-} = Pb(Oxalate)_2^{2-}$

(VIII-6) $Pb^{2+} + CO_3^{2-} = PbCO_3(aq)$

(VIII-7) $Pb^{2+} + 2CO_3^{2-} = Pb(CO_3)_2^{2-}$

(VIII-8) $Pb^{2+} + CO_3^{2-} + Cl^- = Pb(CO_3)Cl^-$

(VIII-9) $Pb^{2+} + H_2O(l) \rightleftarrows PbOH^+ + H^+$

(VIII-10) $Pb^{2+} + 2H_2O(l) \rightleftarrows Pb(OH)_2(aq) + 2H^+$

(VIII-11) $Pb^{2+} + 3H_2O(l) \rightleftarrows Pb(OH)_3^- + 3H^+$

(VIII-12) $PbB_4O_7(aq) + 9H_2O(l) \rightleftarrows Pb^{2+} + 4B(OH)_4^- + 2H^+$

(VIII-13) $PbB(OH)_4^+ \rightleftarrows Pb^{2+} + B(OH)_4^-$

(VIII-14) $Pb[B(OH)_4]_2(aq) \rightleftarrows Pb^{2+} + 2B(OH)_4^-$

(VIII-15) $Pb^{2+} + EDTA^{4-} = PbEDTA^{2-}$

(VIII-16) $Pb^{2+} + Citrate^{3-} = PbCitrate^-$

(VIII-17) $PbOxalate(cr) = Pb^{2+} + Oxalate^{2-}$

(VIII-18) $PbCO_3(cerussite) = Pb^{2+} + CO_3^{2-}$

(VIII-19) $PbO(litharge) + 2H^+ = Pb^{2+} + H_2O$

(VIII-20) $Pb(BO_2)_2 \cdot H_2O + 3H_2O(l) \rightleftarrows Pb^{2+} + 2B(OH)_4^-$

EPA Comment

3-C-4. Exclusion of Experimental Data with Borate from Am(III) Solubility Uncertainty Analysis. *Brush and Domski (2013) used their Criterion G-9 to select data for the actinide solubility uncertainty analysis; Criterion G-9 specifies that experimental solubility data should be excluded if the solutions contained dissolved elements or species for which μ^0/RT[1] data or Pitzer parameters were not included in the EQ3/6 database (DATA0.FM1). The application of this criterion was reasonable when the experiments included species that are not present in the WIPP repository, for example, when it was used to exclude the Th(IV) experimental data of Colás et al. (2011) because of gluconate in the experimental solutions. However, Brush and Domski (2013) used the presence of borate in GWB and ERDA-6 to exclude solubility data that were obtained in mildly basic WIPP brines. The undeclared assumption for this exclusion would be an admission that the current Am(III) model is inadequate for predicting solubilities in WIPP brines at anticipated repository pcH values. A revised uncertainty analysis for Am(III) must be performed by DOE after the following items have been completed: 1) The Am(III)-tetraborate stability constant and Pitzer parameter data have been incorporated and other appropriate updates have been made to the EQ3/6 database (which satisfy Comments 3-C-3 and 3-C-4) and , 2) Solubility data obtained in mildly basic WIPP brines, such as the Khalili et al. (1994) solubility results have be included in the database.*

Brush, L.H., and P.S. Domski. 2013. Uncertainty analysis of actinide solubilities for the WIPP CRA-2014 PA, Rev. 1. Supersedes ERMS 559278.

Colás, E., M. Grivé, I. Roho and L. Duro. 2011. Solubility of $ThO_2 \cdot xH_2O(am)$ in the presence of gluconate. Radiochimica Acta 99:269-273.

Khalili, F.I., V. Symeopoulos, J.-F. Chen and G.R. Choppin. 1994. Solubility of Nd in brine. Radiochimica Acta 66/67:51-55.

---

[1] *The μ^0/RT value is used in the FMT database, but log K is used in the EQ3/6 database, so Criterion G-9 should cite the log K value*

DOE Response

DOE has performed a revised uncertainty analysis for An(III) (Xiong and Domski 2015) using DATA0.FM2 and a new uncertainty distribution for An(III) has been created. DOE has updated the WIPP EQ3/6 database with the special reference to address EPA Comment 3-C-3 (Xiong and Domski 2016). The updated database (DATA0.FM2) includes the thermodynamic and Pitzer parameters derived from the experimental work regarding:

- Hydromagnesite (Xiong 2011), log K = 29.3328 [see details in Xiong and Domski (2016)]
- Lead chemistry species (Xiong 2013a) [for complete lead chemistry species entries for DATA0.FM2, please see Xiong and Domski (2016)]
- Borate chemistry species (Xiong 2013b) [for complete borate chemistry species entries for DATA0.FM2, please see Xiong and Domski (2016)]
- The stability constant for the Am(III)-tetraborate complex, $AmHB_4O_7^{2+}$, and its associated Pitzer parameters (Xiong 2015) parameterized from the data for Nd(III) (Borkowski et al. 2010), log K = –37.34 [see details in Xiong and Domski (2016)]
- The data for the Am(III)-EDTA complex (Xiong 2012, 2013c; Thakur et al. 2014), log K = -20.55 [see details in Xiong and Domski (2016)].

With regard to the solubility experiments performed in mildly basic WIPP brines containing boron, specifically those from Khalili et al. (1994), the solubility controlling phase was determined to be

$Nd(OH)_3 \cdot nH_2O(am)$. Currently, this phase is missing from both DATA0.FM1 and DATA0.FM2. Thus, the Khalili et al. (1994) data violate Criterion G9 and therefore have not been included in the revised uncertainty analysis with DATA0.FM2.

The results with ERDA-6 containing borate from Rao et al. (1999) were included in the revised uncertainty analysis for Am(III) using the updated database (DATA0.FM2), per our response to EPA Comment 3-C-4.

References:

Borkowski, M., M. Richmann, D.T. Reed, and Y. Xiong. 2010. Complexation of Nd(III) with tetraborate ion and its effect on actinide(III) solubility in WIPP brine. Radiochimica Acta 98:577-582.*

Khalili, F.I., V. Symeopoulos, J.-F. Chen, and G.R. Choppin. 1994. Solubility of Nd in brine. Radiochimica Acta 66/67:51-55.*

Rao, L., D. Rai, A.R. Felmy, and C.F. Novak. 1999. Solubility of $NaNd(CO_3)_2 \cdot 6H_2O(c)$ in Mixed Electrolyte (Na-Cl-CO_3-HCO_3) and Synthetic Brine Solutions, Actinide Speciation in High Ionic Strength Media: Experimental and Modeling Approaches to Predicting Actinide Speciation and Migration in the Subsurface. Proceedings of an American Chemical Society Symposium on Experimental and Modeling Studies of Actinide Speciation in Non-Ideal Systems, Held August 26-28, 1996, in Orlando, Florida. Eds. D.T. Reed, S.B. Clark, and L. Rao. New York, NY: Kluwer Academic/Plenum Publishers. 153-169.*

Thakur, P., Y. Xiong, M. Borkowski, and G.R. Choppin. 2014. Improved thermodynamic model for interaction of EDTA with trivalent actinides and lanthanide to ionic strength of 6.60 m. Geochimica et Cosmochimica Acta 133:299-312.*

Xiong, Y.-L. 2011. Experimental determination of solubility constant of hydromagnesite (5424) in NaCl solutions up to 4.4 m at room temperature. Chemical Geology 284:262-269.*

Xiong, Y.-L. 2012. Sandia National Laboratories Waste Isolation Pilot Plant (WIPP) Analysis Plan AP-134, Revision 3, Analysis Plan for Derivation of Pitzer Parameters in Support of Experimental Work at LANL-CO. ERMS 557474. Sandia National Laboratories, Carlsbad, NM.

Xiong, Y.-L. 2013a. Sandia National Laboratories Waste Isolation Pilot Plant (WIPP) Analysis AP-154, Revision 2, Analysis Plan for Derivation of Thermodynamic Properties Including Pitzer Parameters for Solubility Studies of Iron, Lead and EDTA. ERMS 561114. Sandia National Laboratories, Carlsbad, NM.

Xiong, Y.-L. 2013b. Sandia National Laboratories Waste Isolation Pilot Plant (WIPP) Analysis AP-155, Revision 2, Analysis Plan for Derivation of Thermodynamic Properties Including Pitzer Parameters for Solubility Studies of Borate. ERMS 561392. Sandia National Laboratories, Carlsbad, NM.

Xiong, Y.-L. 2013c. Calculations of Thermodynamic Parameters in EDTA System for Experimental Data from Carlsbad Environmental Monitoring and Research Center (CEMRC). Memo to WIPP Records Center. ERMS 560761. Sandia National Laboratories, Carlsbad, NM.

* Copyrighted reference not provided in Enclosure 2.

Xiong, Y.-L. 2015. Modeling Equilibrium Constant for $AmHB_4O_7^{2+}$ by Reevaluation of the Nd(III) Data for $NdHB_4O_7^{2+}$, and its Associated Pitzer Parameters to be Consistent with the WIPP Thermodynamic Model. ERMS 564857. Sandia National Laboratories, Carlsbad, NM.

Xiong, Y.-L., and P.S. Domski. 2015. Uncertainty Analysis of Actinide Solubilities in Response to EPA Completeness Comments 3-C-4 and 3-C-5 for CRA 2014. ERMS 565125. Sandia National Laboratories, Carlsbad, NM.

Xiong, Y.-L., and P.S. Domski. 2016. Updating the WIPP Thermodynamic Database, Revision 1, Supersedes ERMS 565730. Analysis Report for AP-173, Revision 1. ERMS 566047. Sandia National Laboratories, Carlsbad, NM.

EPA Comment

3-C-5. Am(III) Solubility Uncertainty Distribution. *Brush and Domski (2013) used 172 solubility measurements to determine the Am(III) solubility uncertainty distribution:*

- *109 values from Borkowski et al. (2009)*
- *56 values from Neck et al. (2009)*
- *6 values from Runde and Kim (1995)*
- *1 value from Rao et al. (1999)*

Consequently, the majority of the solubility measurements used to calculated the Am(III) solubility uncertainty distribution were from Borkowski et al. (2009). Brush and Domski (2013) established Criterion G7 for the selection of data for actinide solubility uncertainty analysis; Criterion G7 states that experimental results should be included only if the solubility-controlling solid phase was characterized. As previously noted during review of the PABC-2009 (EPA 2010), inclusion of the Nd(III) solubility data from Borkowski et al. (2009) in the uncertainty analysis is inconsistent with Criterion G7 because only indirect means were used to characterize the solid phases. In fact, modeling calculations carried out during the PABC-2009 review predicted different solid phases than those indirectly determined under some conditions (EPA 2010). As previously observed in the Technical Support Document for the CRA-2009 PABC (EPA 2010), including the Borkowski et al. (2009) data in the uncertainty evaluation significantly decreased the mean concentration of the +III actinides used in PA and will lead to non-conservative predicted +III actinide concentrations. DOE must exclude the Borkowski et al. (2009) data when the Am(III) uncertainty distribution is recalculated after completion of the EQ3/6 database update (see Comment 3-C-3, above).

Borkowski, M., J.-F. Lucchini, M.K. Richmann and D.T. Reed. 2009. Actinide (III) solubility in WIPP Brine, Data Summary and Recommendations. Los Alamos National Laboratory, LCO-ACP-08, LA-14360.

Brush L.H., and P.S. Domski. 2013. Uncertainty analysis of actinide solubilities for the WIPP CRA-2014 PA, Rev. 1. Supersedes ERMS 559278.

EPA (U.S. Environmental Protection Agency). 2010. Technical Support Document for Section 194.24, Evaluation of the Compliance Recertification Actinide Source Term, Backfill Efficacy and Culebra Dolomite Distribution Coefficient Values (Revision1), Docket A-98-49, Item II-B1-25, November 2010.

Neck , V., M. Altmaier, T. Rabung, J. Lützenkirchen and T. Fanhänel. Thermodynamics of trivalent actinides and neodymium in NaCl, MgCl2, and CaCl2 solutions: Solubility, hydrolysis, and ternary Ca-M9III)-OH complexes. Pure and Applied Chemistry 81:1555-1568.

Rao, L., D. Rai, A.R. Felmy and C.F. Novak. 1999. Solubility of NaNd(CO3)3•6H2O(c) in mixed electrolyte (Na-Cl-CO3-HCO3) and synthetic brine solutions. In Actinide Speciation in High Ionic Strength Media: Experimental and Modeling Approaches to Predicting Actinide Speciation and Migration in the Subsurface. Proceedings of an American Chemical Society Symposium on Experimental and Modeling Studies of Actinide Speciation in Non-Ideal Systems. Held August 26-28, 1996 in Orlando, Florida. Eds. D.T. Reed, S.B. Clark and L. Rao. Kluwer Academic/Plenum Publishers, pp. 153-169.

Runde, W., and J.I. Kim. 1995. Untersuchungen der Übertragbarkeit von Labordaten Natürliche Verhältnisse: Chemisches Verhalten von Drei- und Fünfwertigem Americium in Salinen NaCl-Lösungen (Study of the Extrapolability of Laboratory Data to Natural Conditions: Chemical Behavior of Trivalent and Pentavalent Americium in Saline NaCl Solutions). RCM-01094, Institute for Radiochemistry, Technical University of Munich, Munich, Federal Republic of Germany, ERMS 241862.

DOE Response

DOE agrees that the use of data from Borkowski et al. (2009) does not meet the G7 criterion in the current uncertainty distribution selection criteria. It is also recognized that the weighting of this WIPP-specific data may have overly influenced the distribution established for the CRA 2014 PA.

DOE has updated the WIPP EQ3/6 database in response to EPA Comment 3-C-3 (Xiong and Domski 2016). The updated database (DATA0.FM2) includes the thermodynamic and Pitzer parameters derived from the experimental work regarding hydromagnesite (Xiong 2011), lead species (Xiong 2013a), and borate species (Xiong 2013b), the stability constant for the Am(III)-tetraborate complex, $AmHB_4O_7^{2+}$, and its associated Pitzer parameters (Xiong 2015) parameterized from the data for Nd(III) (Borkowski et al. 2010), and data for the Am(III)-EDTA complex (Xiong 2012, 2013c; Thakur et al. 2014). A revised uncertainty analysis for An(III), with the data from Borkowski et al. (2009) being eliminated, has been performed using the updated database (Xiong and Domski, 2015), and a new uncertainty distribution for An(III) has been created (Xiong and Domski 2015). The data from Borkowski et al. (2009) were not included in the revised uncertainty analysis because they violate Criterion G7. After the exclusion of the data from Borkowski et al. (2009), the mean value of the sampled uncertainty factor for Am(III) is $10^{0.700}$ = 5.012 (Xiong and Domski 2015). Therefore, the mean value of the logarithm of the sampled uncertainty factor used to adjust the baseline Am(III) solubilities are 0.700 (Xiong and Domski 2015). In comparison, the mean value of the sampled uncertainty factor for Am(III) was $10^{-0.678}$ = 0.210 (Brush and Domski 2013), when the data from Borkowski et al. (2009) were included.

References:

Borkowski, M., J.-F. Lucchini, M.K. Richmann and D.T. Reed. 2009. Actinide (III) Solubility in WIPP Brine, Data Summary and Recommendations. LCOACP-08, LA-14360. Los Alamos National Laboratory, Los Alamos, NM.

Borkowski, M., M. Richmann, D.T. Reed, and Y. Xiong. 2010. Complexation of Nd(III) with tetraborate ion and its effect on actinide(III) solubility in WIPP brine. Radiochimica Acta 98:577-582.*

Brush, L.H., and P.S. Domski. 2013. Uncertainty Analysis of Actinide Solubilities for the WIPP CRA-2014 PA, Rev. 1, Supersedes ERMS 559278. Analysis report, February 22, 2013. ERMS 559712. Sandia National Laboratories, Carlsbad, NM.

Thakur, P., Y. Xiong, M. Borkowski and G.R. Choppin. 2014. Improved thermodynamic model for interaction of EDTA with trivalent actinides and lanthanide to ionic strength of 6.60 m. Geochimica et Cosmochimica Acta 133:299-312.*

Xiong, Y.-L. 2011. Experimental determination of solubility constant of hydromagnesite (5424) in NaCl solutions up to 4.4 m at room temperature. Chemical Geology 284:262-269.*

Xiong, Y.-L. 2012. Sandia National Laboratories Waste Isolation Pilot Plant (WIPP) Analysis Plan AP-134, Revision 3, Analysis Plan for Derivation of Pitzer Parameters in Support of Experimental Work at LANL-CO. ERMS 557474. Sandia National Laboratories, Carlsbad, NM.

* Copyrighted reference not provided in Enclosure 2.

Xiong, Y.-L. 2013a. Sandia National Laboratories Waste Isolation Pilot Plant (WIPP) Analysis AP-154, Revision 2, Analysis Plan for Derivation of Thermodynamic Properties Including Pitzer Parameters for Solubility Studies of Iron, Lead and EDTA. ERMS 561114. Sandia National Laboratories, Carlsbad, NM.

Xiong, Y.-L. 2013b. Sandia National Laboratories Waste Isolation Pilot Plant (WIPP) Analysis AP-155, Revision 2, Analysis Plan for Derivation of Thermodynamic Properties Including Pitzer Parameters for Solubility Studies of Borate. ERMS 561392. Sandia National Laboratories, Carlsbad, NM.

Xiong, Y.-L. 2013c. Calculations of Thermodynamic Parameters in EDTA System for Experimental Data from Carlsbad Environmental Monitoring and Research Center (CEMRC). Memo to WIPP Records Center. ERMS 560761. Sandia National Laboratories, Carlsbad, NM.

Xiong, Y.-L. 2015. Modeling Equilibrium Constant for $AmHB_4O_7^{2+}$ by Reevaluation of the Nd(III) Data for $NdHB_4O_7^{2+}$, and its Associated Pitzer Parameters to be Consistent with the WIPP Thermodynamic Model. ERMS 564857. Sandia National Laboratories, Carlsbad, NM.

Xiong, Y.-L., and P.S. Domski. 2015. Uncertainty Analysis of Actinide Solubilities in Response to EPA Completeness Comments 3-C-4 and 3-C-5 for CRA 2014. ERMS 565125. Sandia National Laboratories, Carlsbad, NM.

Xiong, Y.-L., and P.S. Domski. 2016. Updating the WIPP Thermodynamic Database, Revision 1, Supersedes ERMS 565730. Analysis Report for AP-173, Revision 1. ERMS 566047. Sandia National Laboratories, Carlsbad, NM.

EPA Comment

4-(14)15-1. Plan View of the Repository with Updated Dimensions. *The repository layout has changed since the 2009 recertification. Please provide a plan view of the repository design. This should include the dimensions and locations of the repository and should provide the dimensions of the current and planned excavated areas and the run-of-mine salt panel closure system.*

DOE Response

The locations of the run-of-mine salt panel closures are shown in Figure 1. The panel closures are planned to be 100 feet in length. The planned width and height of the panel closures can be found in the Attachment 1 spreadsheet. This is consistent with the Panel Closure System design included in EPA's October 8, 2014, Panel Closure Redesign rulemaking (EPA 2014).

A plan view drawing of the repository that has dimensions for all current and planned excavated areas and run-of-mine salt panel closure systems would be very busy and difficult to read. As a compromise and with the concurrence of EPA staff, the spreadsheet entitled "Mined Volume Sept15 110315," with all the requested dimensions and locations, is provided as Attachment 1 in Enclosure 2. The dimensions in this spreadsheet are based on design excavation openings. Panel closure design dimensions and locations may change over the lifetime of the repository, and are shown on this schematic as planned only. Vertical closure of mined openings in the WIPP underground historically ranges from one inch per year to over six inches per year depending on location and size of the opening (DOE 2015). The design excavation dimensions provide a reasonable approximation to the as-built system, considering the ongoing processes of creep closure and maintenance of access mains and other sections of the underground facility. In addition, a NWP drawing (ENG-15-004) that shows the current repository design and the locations cited in the spreadsheet is shown in Figure 1.

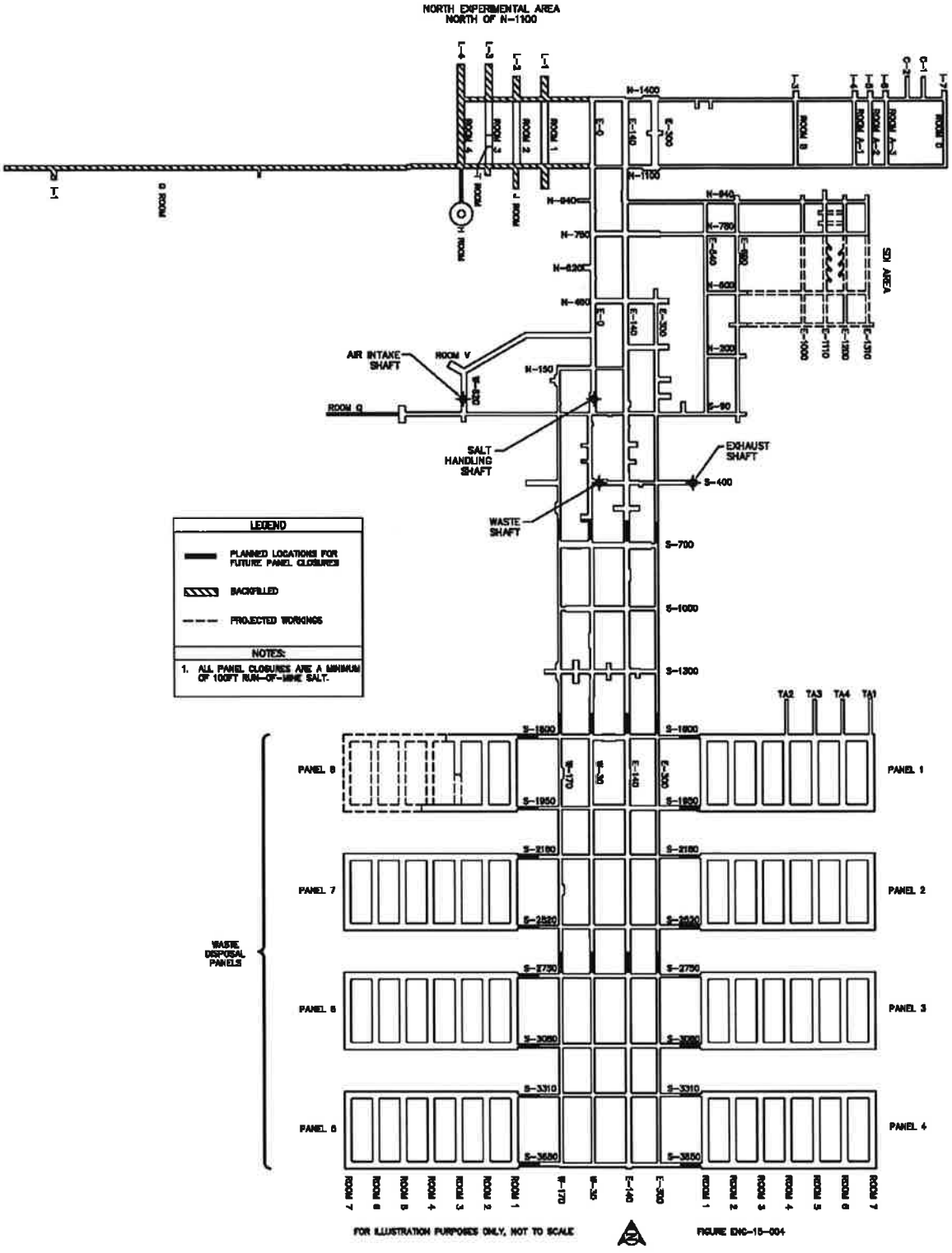
NORTH EXPERIMENTAL AREA
NORTH OF N-1100
AIR INTAKE SHAFT
ROOM V
ROOM Q
SALT HANDLING SHAFT
EXHAUST SHAFT
WASTE SHAFT
LEGEND
PLANNED LOCATIONS FOR FUTURE PANEL CLOSURES
BACKFILLED
PROJECTED WORKINGS
NOTES:
1. ALL PANEL CLOSURES ARE A MINIMUM OF 100FT RUN-OF-MINE SALT.
WASTE DISPOSAL PANELS
PANEL 8
PANEL 7
PANEL 6
PANEL 5
PANEL 1
PANEL 2
PANEL 3
PANEL 4
FOR ILLUSTRATION PURPOSES ONLY, NOT TO SCALE
FIGURE ENC-15-004

Figure 1

References:

Economy, K. 2015. Email to Steve Kouba (Subject: EPA Question 4-(14)15-1). September 21, 2015.

U.S. Department of Energy (DOE). 2015. Waste Isolation Pilot Plant Geotechnical Analysis Report for July 2013 – June 2014. DOE/WIPP 15-3556. Carlsbad Field Office, Carlsbad, NM.

U.S. Environmental Protection Agency (EPA). 2014. 40 CFR Part 194: Criteria for the Certification and Recertification of the Waste Isolation Pilot Plant's Compliance with the Disposal Regulations; Panel Closure Redesign. Federal Register, Vol. 79, No. 195, 60750 – 60756. October 8, 2014.

EPA Comment

4-C-2. Reassessment of Inundated Anoxic Steel Corrosion Rate Data.

a. ***Experimental Data Used As Inputs For Parameter CORRMCO2*** *– The DOE needs to justify the values it has adopted for the parameter CORRMCO2 given the range of existing data. In the CRA-2014 PA the parameter CORRMCO2 has a range, distribution and median value that was modified from what was adopted in the CCA. The modification was based on experimental corrosion data under inundated conditions, at 1 atm and 0 ppm CO_2, as reported in Roselle (2013). Repository brines are predicted to be in equilibrium with CO_2 gas concentrations of 3.2 ppm CO_2 ($10^{-5.5}$ atm, Brush and Domski 2013) which is above 0 ppm CO_2. Additional corrosion experiments were performed by Roselle at CO_2 concentrations of 350 ppm, 1500 ppm and 3500 ppm, with and without organic ligands, and for partially and fully immersed coupons. This range includes the predicted CO_2 gas concentrations of 3.2 ppm. The corrosion rates determined by Roselle (2013) for experiments at 0 and 350 ppm CO_2 concentrations are summarized in the figure below. The collective results from these experiments indicate corrosion does occur above 0 ppm and up to 350 ppm CO_2 and corroborate relevant data that indicates corrosion will occur at CO_2 concentrations above 0 ppm.*

Please provide a justification for why the experimental corrosion data gathered from experiments above 0 ppm CO_2 concentrations were not included in the development of the parameter CORRMCO2.

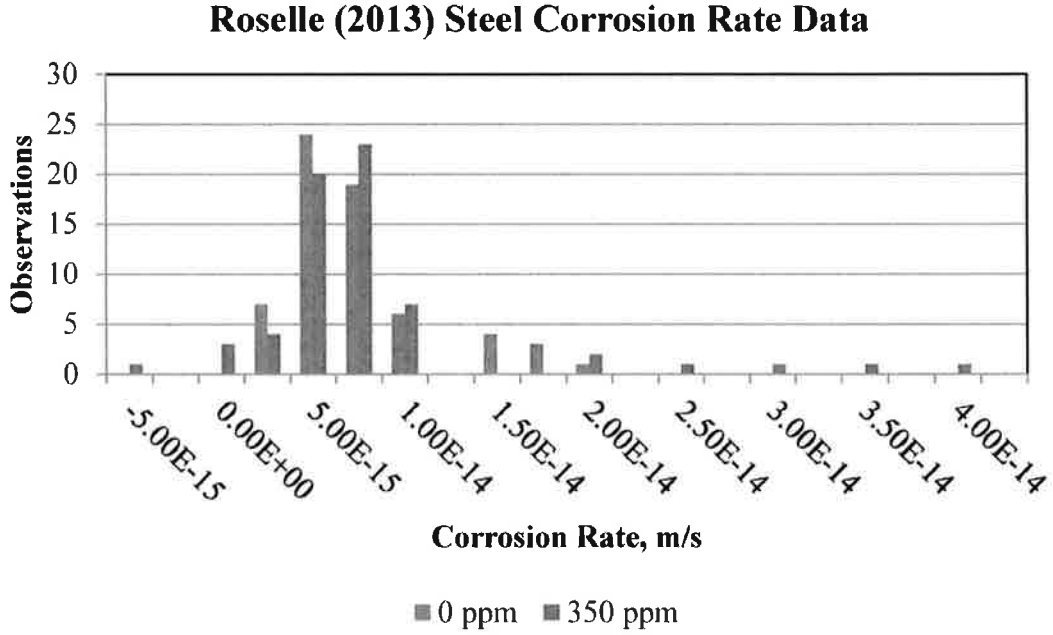

b. ***Justify the Distribution of Parameter CORRMCO2*** *– In previous WIPP PAs, the lower limit of the steel corrosion rates was set equal to 0 m/sec, and, accordingly, the lower limit of the sampled range for CORRMCO2 should be 0 m/s. This lower limit is consistent with passivation of the steel surface by H_2S observed and reported in Telander and Westerman (1997). Telander and Westerman (1993, 1997) reported the results of anoxic corrosion experiments at H_2 and N_2 pressures up to 127 atm, which are applicable given the expected hydrostatic pressures anticipated in the WIPP repository. Based on an experiment with a N_2 pressure of 10 atm, Telander and Westerman (1997) recommended a corrosion rate of 2.24 x 10^{-14} m/s using results*

from the final 12 months of a 24-month experiment. EPA (1998) noted the effects of increased pressure on the steel corrosion rate in the experiments by Telander and Westerman (1993, 1997) and directed that the upper limit for CORRMCO2 used in the CCA PAVT should be increased to 3.17 x 10^{-14} m/s (see Table Parameter CORRMCO2). Retaining this upper limit encompasses most, but not all, of the corrosion rate data measured by Roselle (2013) and includes consideration of the results reported by Telander and Westerman (1993, 1997).

The Roselle (2013) anoxic corrosion experiments with 0 ppm and 350 ppm CO_2 concentrations bracket anticipated CO_2 gas phase concentrations. It appears that the 350 ppm CO_2 corrosion data should have been included in the reassessment of the CORRMCO2 parameter because the experimental data indicate that steel corrosion rate will occur up to 350 ppm CO_2. However, the 350 ppm CO_2 corrosion data were not included in establishing the parameter valuation.

Please update the range, median and distribution for the CORRMCO2 parameter that reflects this experimental data.

Please provide justification as to why a uniform distribution for parameter CORRMCO2 was not adopted in the CRA-2014 PA.

Table Parameter CORRMCO2 (m/s)

WIPP PA	Distribution	Minimum	Maximum	Median
CCA PA	Uniform	0.0	1.59×10^{-14}	7.94×10^{-15}
CCA PAVT CRA-2004 PA and PABC CRA-2009 PA and PABC	Uniform	0.0	3.17×10^{-14}	1.58×10^{-14}
CRA-2014 PA	Student-t	3.29×10^{-16}	1.84×10^{-14}	6.06×10^{-15}

Brush, L.H., and P.S. Domski. 2013. Prediction of Baseline Actinide Solubilities for the WIPP CRA-2014 PA. Sandia National Laboratories, ERMS 559138.

EPA. 1998. Technical Support Document for Section 194.23: Parameter Justification Report. Docket No. A-93-02 V-B-14.

Roselle, G.T. 2013. Determination of Corrosion Rates from Iron/Lead Corrosion Experiments to be Used for Gas Generation Calculations. Sandia National Laboratories, ERMS 559077.

Telander, M.R., and R.E. Westerman. 1993. Hydrogen Generation by Metal Corrosion in Simulated Waste Isolation Pilot Plant Environments: Progress Report for the Period November 1989 Through December 1992. Prepared by Pacific Northwest National Laboratory for Sandia National Laboratory, SAND92-7347.

Telander, M.R., and R.E. Westerman. 1997. Hydrogen Generation by Metal Corrosion in Simulated Waste Isolation Pilot Plant Environments. Prepared by Pacific Northwest National Laboratory for Sandia National Laboratory, SAND96-2538.

DOE Response

a. Based on the EPA comment, DOE has reanalyzed the applicability of data from iron corrosion experiments at 0 and 350 ppm CO_2 (Roselle 2013) to the expected conditions in the WIPP repository. This reanalysis is relevant to determining the STEEL:CORRMCO2 parameter representing anoxic corrosion of brine inundated steel.

Roselle (2013) reported results from inundated and humid experiments, with gas phase CO_2 concentrations of 0 ppm and 350 ppm. For the CRA-2014, Roselle (2013) recommended that the parameter STEEL:CORRMCO2 be changed to reflect the new data from experiments with 0 ppm CO_2, but he did not suggest incorporation of the 350 ppm data. The resulting parameter distribution derived for use in the CRA-2014 PA is listed in Kicker and Herrick (2013), Table 4.

The EPA suggests that the 350 ppm CO_2 data should also be considered in the uncertainty distribution for STEEL:CORRMCO2. Roselle's experiments were conducted at 1 atm and 350 ppm CO_2 which corresponds to a partial pressure of CO_2 of 3.5E-04 atm. The steel corrosion rate is a function of the aqueous concentration of CO_2 (Roselle 2013), which is directly related to the partial pressure of CO_2 by Henry's Law.

Pressure in the repository after closure will be up to lithostatic, i.e., 150 atm. Current PA calculations (with the new thermodynamic database, DATA0.FM2) estimate the fugacity of CO_2 to be 5.8E-07 atm at 1 atm total pressure (Domski and Xiong 2015).[1] Calculation of the fugacity of CO_2 in a repository at 150 atm is not a linear extrapolation, but if it were, the value would be 8.70E-05 atm, much higher than can be expected, but still an order of magnitude below the 3.5E-04 atm in the Roselle experiments. Thus, the partial pressure of CO_2 in the Roselle experiments (i.e., 3.5E-04 atm) exceeds the partial pressure of CO_2 in the repository after closure by at least a factor of 4. The DOE accepts the EPA position that:

> *The Roselle (2013) anoxic corrosion experiments with 0 ppm and 350 ppm CO2 concentrations bracket anticipated CO2 gas phase concentration.*

However, our justification for determining the range of experimental conditions to consider takes into account the overall pressure of the experiments (1 atm) compared to the expected WIPP conditions (150 atm).

It should be noted that magnesium oxide (MgO) is emplaced in the repository to sequester CO_2, resulting in an updated equilibration gas phase concentration with DATA0.FM2 of 0.58 ppm CO_2 (Domski and Xiong 2015). Therefore, the corrosion rates in Roselle (2013) reported for experiments at 1500 ppm and 3500 ppm CO_2 and 1 atm are not viewed as relevant to WIPP conditions.

b. The DOE proposes to update the range, median and distribution for the STEEL:CORRMCO2 parameter to consider experimental data obtained from iron corrosion experiments at 0 and 350 ppm CO_2 (Roselle 2013). Observed rates for experiments at 0 ppm and 350 ppm CO_2 were used (Zeitler and Hansen 2015a, 2015b) to form a cumulative distribution for STEEL:CORRMCO2

[1] The fugacity of CO_2 in the CRA-2014 PA was 3.14 (i.e., a gas-phase concentration of 3.14 ppm) which corresponds to a partial pressure of 4.65E-04 atm given a total pressure of 150 atm (Brush and Domski 2013). However, in response to the EPA CRA-2014 Completeness Comments 3-C-3 and 3-C-4, new baseline solubilities were calculated with the revised EQ3/6 thermodynamic database and an updated fugacity of 0.58 was calculated (Domski and Xiong 2015).

(Figure 1). The cumulative distribution in Figure 1 reflects the observed variation in non-negative corrosion rates for all experiments with 0 ppm and 350 ppm CO_2 with the lower bound value of 0 m/s. The revised distribution considers all non-negative corrosion rates reported by Roselle (2013) as equally likely and is the proposed distribution for STEEL:CORRMCO2.

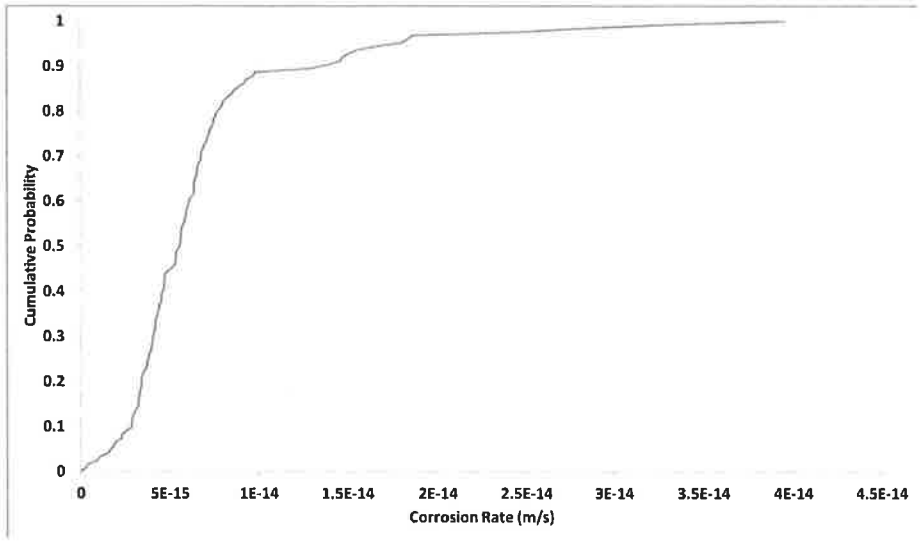

Figure 1. Cumulative distribution function for revised STEEL:CORRMCO2 parameter.

In conclusion, the DOE proposes to modify the STEEL:CORRMCO2 parameter to reflect a cumulative distribution that considers the 0 and 350 ppm experimental results, which DOE believes to bracket the conditions expected in the WIPP (Zeitler and Hansen 2015a, 2015b). The DOE may incorporate the revised distribution in a future PA after further discussion with EPA.

References:

Brush, L.H., and P.S. Domski. 2013. Prediction of Baseline Actinide Solubilities for the WIPP CRA-2014 PA. ERMS 559138. Sandia National Laboratories, Carlsbad, NM.

Domski, P., Y.-L. Xiong. 2015. Prediction of Baseline Actinide Solubilities with an Updated EQ3/6 Thermodynamic Database (DATA0.FM2) in Response to EPA Completeness Comment 3-C-3 for CRA 2014. ERMS 565032. Sandia National Laboratories, Carlsbad, NM.

Kicker, D.C. and C. Herrick. 2013. Parameter Summary Report for the 2014 Compliance Recertification Application (Revision 0). ERMS 560298. Sandia National Laboratories, Carlsbad, NM.

Roselle, G.T. 2013. Determination of Corrosion Rates from Iron/Lead Corrosion Experiments to be used for Gas Generation Calculations (Revision 1). Analysis Report, January 23, 2013. ERMS 559077. Sandia National Laboratories, Carlsbad, NM.

U.S. Department of Energy (DOE). 1996. Title 40 CFR Part 191 Compliance Certification Application for the Waste Isolation Pilot Plant (October). 21 vols. DOE/CAO-1996-2184. Carlsbad Area Office, Carlsbad, NM.

U.S. Department of Energy (DOE). 2014. Title 40 CFR Part 191 Compliance Recertification Application for the Waste Isolation Pilot Plant. DOE/WIPP 2014-3503. DOE Waste Isolation Pilot Plant, Carlsbad Field Office.

Zeitler, T.R. and C. Hansen. 2015a. Cumulative distribution for STEEL:CORRMCO2. ERMS 565005. Sandia National Laboratories, Carlsbad, NM.

Zeitler, T.R. and C. Hansen. 2015b. Supplemental Information to the Cumulative distribution for STEEL:CORRMCO2. ERMS 565104. Sandia National Laboratories, Carlsbad, NM.

EPA Comment

4-C-3. Humid Steel Corrosion Rates. *Roselle (2013) states that steel coupons hung in a humid environment exhibited essentially no corrosion regardless of CO_2 concentration. This statement contradicts the experimental data (reported in Roselle, 2013) conducted under humid experimental conditions, where samples were tested at 0 and 350 ppm CO_2. These experiments indicate corrosion does occur under humid conditions, with a mean corrosion rate of 3.0×10^{-16} m/s and median rate or 1.1×10^{-16} m/s, both positive values. The provided histogram of the corrosion rate data, obtained with gas phase CO_2 concentration of 0 ppm and 350 ppm – which bracket anticipated repository conditions – demonstrates that the humid corrosion rate could be greater than zero.*

Please justify why the DOE does not use the available and WIPP-relevant data in the derivation of corrosion rates that indicate corrosion will occur under humid conditions.

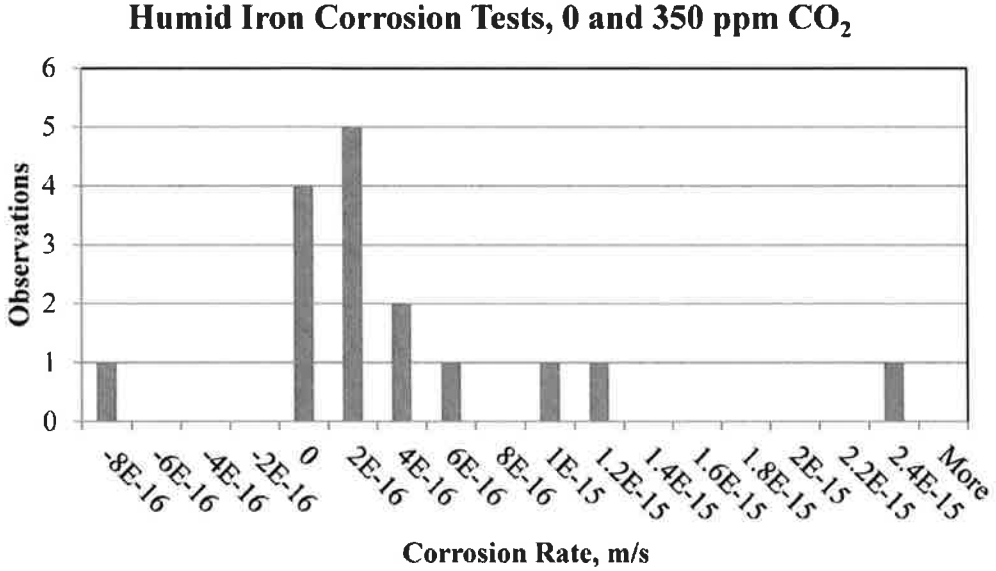

Roselle, G.T. 2013. Determination of Corrosion Rates from Iron/Lead Corrosion Experiments to be Used for Gas Generation Calculations. Sandia National Laboratories, ERMS 559077.

DOE Response

Based on the EPA comment, DOE has reanalyzed the applicability of data from iron corrosion experiments at 0 and 350 ppm CO_2 (Roselle 2013) to the expected conditions in the WIPP repository. This reanalysis is relevant to determining the STEEL:HUMCORR parameter representing anoxic corrosion of steel under humid conditions. The humid steel corrosion rate used in all past compliance performance assessments (PAs) was 0. The justification for this parameter value was given in Wang and Brush (1996) and states:

"The corrosion rate observed on specimens exposed to humid conditions is negligible, based on essentially non-existent presence of corrosion product and lack of apparent H_2 generation (Telander & Westerman, 1995). Therefore, we set the humid steel corrosion rate to 0."

Roselle (2013) reported results from inundated and humid experiments, with gas phase CO_2 concentrations of 0 ppm and 350 ppm. Roselle indicated that some corrosion occurs under simulated WIPP conditions for humid environments. Some experiments were conducted with no CO_2, whereas

others included higher concentrations than are expected in the repository. The selection of corrosion rates based solely on 0 ppm CO_2 experiments may not completely reflect iron corrosion under WIPP conditions because there is a predicted fugacity of 5.8E-07 atm CO_2 at 1 atm total pressure in the gas phase when in equilibrium with WIPP brines (Domski and Xiong 2015).[1] Therefore, it is appropriate to also consider data from corrosion experiments performed under conditions with nonzero CO_2 concentrations. The data available from Roselle (2013) include corrosion rates for CO_2 concentrations of 0 and 350 ppm under humid conditions. A 350 ppm CO_2 concentration in the gas phase is two orders of magnitude higher than the predicted equilibrium concentration, and therefore the 350 ppm data are used with the 0 ppm data to construct a distribution for the STEEL:HUMCORR parameter via linear interpolation between the two data sets, rather than by aggregating the two sets of data (Zeitler and Hansen 2015b).[2]

The humid corrosion rate data in Roselle (2013) comprises 16 data points, 8 for samples tested at 0 ppm CO_2 and 8 for samples tested at 350 ppm CO_2. The 350 ppm CO_2 data set is reduced to four samples by excluding negative corrosion rates. A cumulative distribution function (CDF) is created for each set of data separately, and a CDF representative of corrosion rates at 0.58 ppm CO_2 is formed by linearly interpolating between quantiles (Figure 1). The result is a CDF that can be used as a cumulative distribution to describe the STEEL:HUMCORR parameter (Table 1).

[1] The fugacity of CO_2 in the CRA-2014 PA was 3.14 (Brush and Domski 2013). However, in response to the EPA CRA-2014 Completeness Comments 3-C-3 and 3-C-4, new baseline solubilities were calculated with the revised EQ3/6 thermodynamic database and an updated fugacity of 0.58 was calculated (Domski and Xiong 2015).

[2] A distribution for the STEEL:HUMCORR parameter was previously constructed based on 3.14 ppm CO_2 in the gas phase (Zeitler and Hansen 2015a).

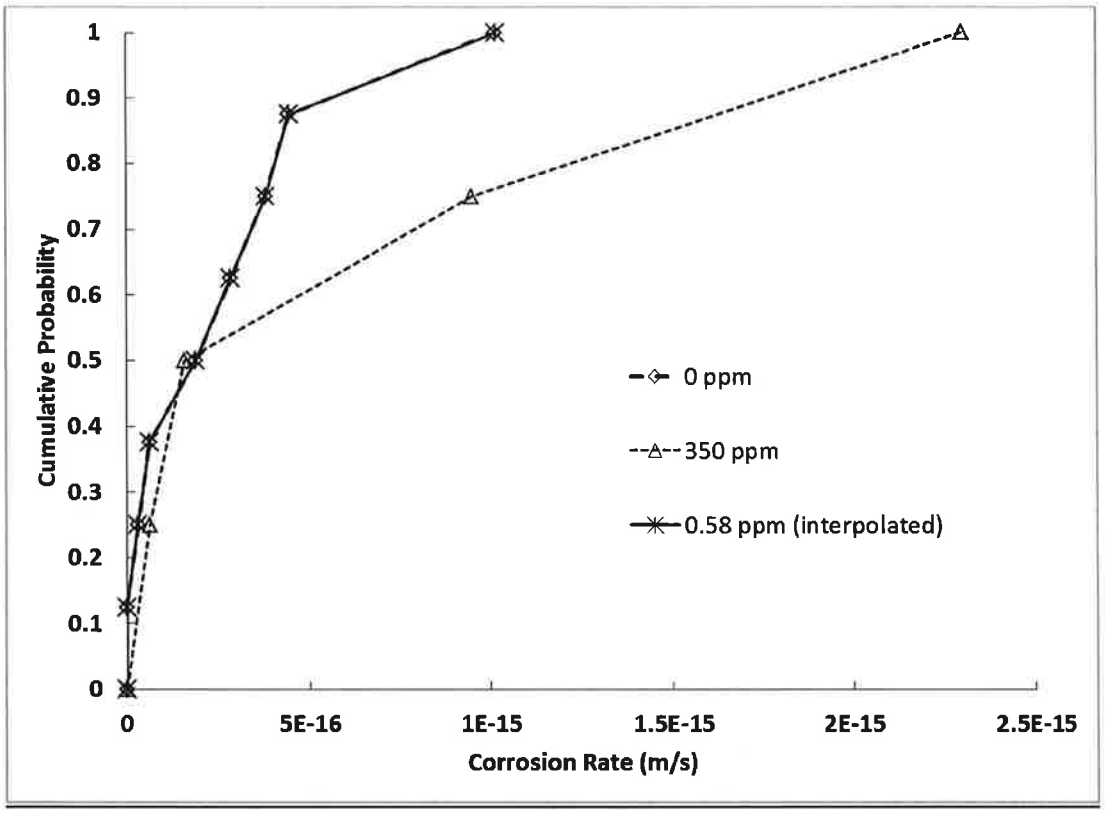

Figure 1. CDFs for the 0 ppm and 350 ppm CO_2 data sets, as well as the final interpolated CDF for 0.58 ppm (Figure 1 from Zeitler and Hansen 2015b).

1

Table 1. CDF data for the STEEL:HUMCORR parameter that describes iron corrosion rates (Table 1 from Zeitler and Hansen 2015b).

Value (m/s)	Cumulative Probability
0	0
5.22E-20	0.125
3.18E-17	0.25
6.35E-17	0.375
1.90E-16	0.5
2.86E-16	0.625
3.81E-16	0.75
4.46E-16	0.875
1.02E-15	1

The DOE may incorporate the revised distribution for the STEEL:HUMCORR parameter into a future PA after further discussion with EPA.

References:

Wang, Y. and L.H. Brush. 1996. Estimate of Gas Generation Parameters for the Long-Term WIPP Performance Assessment. ERMS231943. Sandia National Laboratories, Albuquerque, NM.

Brush, L.H. and P.S. Domski. 2013. Prediction of Baseline Actinide Solubilities for the WIPP CRA-2014 PA. ERMS 559138. Sandia National Laboratories, Carlsbad, NM.

Domski, P., Y.-L. Xiong. 2015. Prediction of Baseline Actinide Solubilities with an Updated EQ3/6 Thermodynamic Database (DATA0.FM2) in Response to EPA Completeness Comment 3-C-3 for CRA 2014. ERMS 565032. Sandia National Laboratories, Carlsbad, NM.

Roselle, G.T. 2013. Determination of Corrosion Rates from Iron/Lead Corrosion Experiments (Revision 1). Analysis Report, January 23, 2013. ERMS 559077. Sandia National Laboratories, Carlsbad, NM.

Zeitler, T.R. and C. Hansen. 2015a. Cumulative distribution for STEEL:HUMCORR. ERMS 565009. Sandia National Laboratories, Carlsbad, NM.

Zeitler, T.R. and C. Hansen. 2015b. Updated calculation of the cumulative distribution for STEEL:HUMCORR. ERMS 565108. Sandia National Laboratories, Carlsbad, NM.

EPA Comment

4-C-6. Effects of Green Rust Formation on Gas Generation Stoichiometry. *The stoichiometric coefficient used in PA for gas generation due to steel corrosion (STOIFX) has been maintained at its historical value of 1. This parameter value of "1" assumes no green rust will form on steel. The assumption is contradicted in Appendix SOTERM Section 2.3.4 of the CRA-2014, which includes the following statement:*

> *Roselle (Roselle 2013) states that green rust is the most likely corrosion product in experiments with low atmospheric CO_2 concentrations (< 350 ppm).*

Roselle (2013 Section 4.3) then contradicts the above statement stating current experiments indicate no evidence that corrosion products will occur on steel under WIPP-relevant conditions. He further claims results from recent experiments are similar to what was observed in the earlier Telander and Westerman (1993) corrosion investigations [$Fe(OH)_2$]. However, corrosion products have been reported by Roselle (2013) in WIPP related experiments and contradicts Roselle's own assumption report in Roselle, 2013 Section 4.3. Archeological evidence indicates corrosion products will occur under harsh anaerobic conditions. Réguer et al. (2007) and Rémazeilles et al. (2009) indicate long term corrosion products have formed on iron artifacts under anaerobic conditions and saline conditions. This is further corroboration that corrosion products, such as green rust, could form on WIPP steel. Production of corrosion products could result in a higher value of STOIFX, as demonstrated in the following equation:

$$6Fe + CO_2 + 15H_2O = Fe_6(OH)_{12}CO_3 \cdot 2H_2O + 7\,H_2$$

Given the contradictions, the DOE should discuss why a value of "1" should be used for the parameter STOIFX. In this discussion, the DOE needs to address all available data, including the solids characterization results from the iron corrosion experiments performed by Roselle (Roselle 2009, 2010, 2011a, 2011b) and analogue data that indicate corrosion occurs in anaerobic and saline high chloride media (e.g., Réguer et al. 2007, Rémazeilles et al. 2009) in the development of the parameter STOIFX.

Réguer, S., P. Dillman and F. Mirambet. 2007. Buried iron archaeological artefacts: corrosion mechanisms related to the presence of Cl-containing phases. Corrosion Science 49:2726-2744.

Rémazeilles, C., D. Neff, F. Kergourlay, E. Foy, E. Conforto, S. Reguer, P. Refait and P. Dillmann. 2009. Mechanisms of long-term anaerobic corrosion of iron archaeological artefacts in seawater. Corrosion Science 51:2932-2041.

Roselle, G.T. 2009. Iron and Lead Corrosion in WIPP-Relevant Conditions: Six Month Results. Milestone report, October 7, 2009, Sandia National Laboratories, ERMS 546084.

Roselle, G.T. 2010. Iron and Lead Corrosion in WIPP-Relevant Conditions: 12 Month Results. Milestone report, October 14, 2010, Sandia National Laboratories, ERMS 554383.

Roselle, G.T. 2011a. Iron and Lead Corrosion in WIPP-Relevant Conditions: 18 Month Results. Milestone report, May 3, 2011, Sandia National Laboratories, ERMS 555246.

Roselle, G.T. 2011b. Iron and Lead Corrosion in WIPP-Relevant Conditions: 24 Month Results. Milestone report, January 5, 2011, Sandia National Laboratories, ERMS 554715.

Roselle, G.T. 2013. Determination of Corrosion Rates from Iron/Lead Corrosion Experiments to be Used for Gas Generation Calculations. Sandia National Laboratories, ERMS 559077.

Telander, M.R., and R.E. Westerman. 1993. Hydrogen Generation by Metal Corrosion in Simulated Waste Isolation Pilot Plant Environments: Progress Report for the Period November 1989 Through December 1992. Prepared by Pacific Northwest National Laboratory for Sandia National Laboratory, SAND92-7347.

DOE Response

1. Introduction

The primary corrosion mechanism for steel exposed to WIPP brines and/or humid WIPP air is

$$Fe + 2H_2O = Fe(OH)_2 + H_2 \quad (1)$$

Other possible corrosion mechanisms may exist but are believed to be of much lesser importance than the mechanism shown in Equation 1. Based on the stoichiometry in Equation 1, one mole of hydrogen is produced for each mole of Fe that is corroded.

2. The Primary Corrosion Mechanism

The dominant corrosion product under anoxic, chloride-enriched conditions in the WIPP is $Fe(OH)_2$ or its successor, Fe-hibbingite, $Fe(II)_2(OH)_3Cl(cr)$, both being Fe(II) products, and will therefore retain the 1:1 stoichiometry ratio for Fe to H_2. DOE maintains that the molar ratio of hydrogen gas to iron should be 1 given anoxic corrosion of iron in the absence of CO_2. Appendix SOTERM 2.3.4 of the CRA-2014 incorrectly references Roselle (2013) as stating that green rust dominates at less than 350 ppm CO_2. In fact, Roselle (2013) states that $Fe(OH)_2$ is the most likely corrosion product in experiments with low atmospheric CO_2 concentrations (even at 350 ppm CO_2).

The STOIFX parameter is based on the predominant mechanism for steel corrosion based on experiments performed by Telander and Westerman (1993 and 1997) and Roselle (2009, 2010, 2011a, 2011b, and 2013). The parameter STOIFX [X_C (H_2 | Fe) = 1 mole H_2 per mole Fe (Kicker and Herrick 2013)] represents the stoichiometric coefficient for hydrogen gas generation due to the anoxic corrosion of steel. This is based on the following assumptions/conditions in the WIPP repository:

a) Microbially produced carbon dioxide (CO_2) will largely be removed by reaction with the magnesium oxide (MgO) backfill (DOE/CAO 1996-2184, WCA).
b) Anoxic conditions will be dominant during the regulatory period of 200-10,000 years.
c) Significant partial pressures of hydrogen sulfide (H_2S) are not expected, based on WIPP-specific data that show that passivation does not occur at low CO_2 levels (Telander and Westerman 1993 and 1997, Roselle 2013).
d) Reducing conditions exist in the repository.

Under the conditions defined by (a) through (d) above, the interaction of steel in WIPP with repository brines has been shown to result in the formation of H_2 gas depending on the corrosion rate and the type of corrosion products formed. As written in CCA-1996 and based on observations of Telander and Westerman (1993), the predominant and mostly likely corrosion product of steel in the absence of CO_2 is $Fe(OH)_2$, as indicated by Reaction 1.

In the reducing environments expected at WIPP, reduced iron phases (Fe(II) oxides and zero valent iron) and aqueous ferrous iron will be present. These are all reducing agents towards key actinide species (see SOTERM 2014, Table SOTERM-3) and will help establish the predominance of lower-valent actinides in the WIPP. Given the high concentrations of chloride in WIPP brines, ferrous hydroxide

would be transformed to Fe-hibbingite. Fe-hibbingite will control the solubility of iron, leading to a predicted solubility on the order of ~10^{-3} m for pH between 8.5 and ~9 (Nemer et al. 2011).

3. Other Possible Corrosion Mechanisms in WIPP

Experiments reported by Telander and Westerman (1993, 1997) investigated gas generation from corrosion under a wide range of possible conditions in the repository. The studies included corrosion of low-carbon steel waste packaging materials in synthetic brines, representative of intergranular Salado brines at the repository horizon, under anoxic (reducing) conditions.

WIPP-specific experiments have shown that steels and other Fe-based alloys could corrode by mechanisms in addition to reaction 1, possibly like that shown in Reaction 2 (the formation of magnetite).

$$3Fe + 4H_2O = Fe_3O_4 + 4H_2 \quad (2)$$

When normalized to 1 mole of Fe and linearly weighted by the factors x and 1-x ($0 \leq x \leq 1$), the reactions (1) and (2) become

$$Fe + \left(\frac{4+2x}{3}\right)H_2O = \left(\frac{4-x}{3}\right)H_2 + xFe(OH)_2 + \left(\frac{1-x}{3}\right)Fe_3O_4 \quad (3)$$

where x and (1-x) are the fractions of Fe consumed in the reactions in Equation (1) and Equation (2), respectively. Although magnetite (Fe_3O_4) has been observed to form as a corrosion product at elevated temperatures in oxic brine (Haberman and Frydrych 1988), there is no evidence that it will form as a predominant product at WIPP repository temperatures and WIPP anoxic conditions. If Fe_3O_4 were to form as seen in Reaction 2, H_2 would be produced (on a molar basis) in excess of the amount of Fe consumed. However, anoxic corrosion experiments (Telander and Westerman 1993) did not indicate the production of H_2 in excess of the amount of Fe consumed. Therefore, the stoichiometric factor x in Reaction 3 was set to 1.0 (i.e., $x = 1$), which implies that Reaction 1 represents corrosion.

Furthermore, researchers have noted that after $Fe(OH)_2$ is formed it can be transformed by two different reaction paths as shown in Reactions 4 and 5.

$$3Fe(OH)_2 = Fe_3O_4 + H_2 + 2H_2O \quad (4)$$

$$2Fe(OH)_2 + Cl^- + H^+ = Fe(II)_2(OH)_3Cl(cr) + H_2O \quad (5)$$

However, WIPP-specific experiments conducted by Nemer et al. (2011) indicate that iron hydroxide reacts with high chloride brines to form iron hibbingite, $Fe(II)_2(OH)_3Cl(cr)$, according the Equation 5. This is because in environments where there are relatively high concentrations of chloride, like that of the WIPP brines (e.g., 6.40 m Cl^- in GWB, and 5.27 m Cl^- in ERDA-6; Xiong and Lord 2008), the reaction shown in Equation 5 is favored over the reaction shown in Equation 4. The reader should note that in the case of Equation 5, there is no hydrogen gas produced. Thus, the stoichiometric factor for corrosion producing hydrogen gas is still 1 ($x = 1$) as indicated by Equation 6.

$$X_c(H_2|Fe) = \frac{(4-x)}{3} = \frac{1\ \text{mol}}{\text{mol}} \quad (6)$$

Metallic iron can also be corroded into $FeCO_3$ or FeS. In both cases, the stoichiometric ratio of hydrogen gas produced to iron corroded is also 1 to 1.

Regarding the potential formation of green rust, the structure and composition of green rust has been widely documented (e.g., Refait et al. 1998, Génin et al. 2001, Ruby et al. 2003, Simon et al. 2003). Despite the increasing knowledge of green rust formation mechanisms, and of the evident interactions between green rust and metals or contaminants, little is known about the surface chemistry and evolution of green rust particles in aqueous media.

Roselle (2013) determined corrosion rates for steel inundated in brine in the absence of CO_2. The objective of Roselle's work was to determine: (a) the extent to which steel consumes CO_2 via the formation of carbonates or other phases, potentially supporting MgO in CO_2 sequestration; and (b) determining hydrogen gas generation rates based on measured corrosion rates. The determination of the corrosion products of the first objective in Roselle's final report has not been completed.

The study conducted by Roselle's steel coupons did show formation of several phases dependent on the partial pressure of CO_2 (P_{CO2}). Scanning electron microscope (SEM) analysis with energy dispersive spectroscopy (EDS) showed the presence of a green Fe (±Mg) chlorhydroxide phase at P_{CO2} values <1500 ppm. At higher P_{CO2} the dominant corrosion product was a Fe-Mg-Ca hydroxicarbonate phase. In general, his experiments showed corrosion rates increasing as a function of increasing CO_2 concentrations. In the analysis work, Roselle (2013) expanded his conclusions saying: "It is possible that other corrosion products (e.g., green rust, hibbingite, etc.) may also form (Nemer et al., 2011)." Largely, green rust, although formed, is not the major product, and is transient in nature between metallic iron and the final corrosion product(s) (Refait et al. 1998).

This is supported by Nemer et al. (2011) who concluded that when low-carbon steel interacts with chloride-rich anoxic brine, the phase $Fe(II)_2(OH)_3Cl(cr)$, which is the pure-iron end member of hibbingite $(Fe^{II}, Mg)_2(OH)_3Cl(s)$, is likely to buffer the oxygen fugacity in the repository and is also expected to be a likely corrosion product in addition to some transient green rust containing sulfate. The anoxic corrosion of iron in chloride-rich brines to form the pure-iron end member of hibbingite, the likely final product, can be expressed as the following overall reaction and still retains the 1:1 stoichiometry ratio for Fe to H_2,

$$2Fe(cr) + 3H_2O(l) + Cl^- + H^+ = Fe(II)_2(OH)_3Cl(cr) + 2H_2(g) \quad (7)$$

It is worth noting that iron hydroxychlorides (β and γ-$Fe_2(OH)_3Cl$) are also observed in chloride-rich environments when iron archaeological artifacts were corroded (Neff et al. 2005; Réguer et al. 2007; Bellot-Gurlet et al. 2009; Rémazeilles et al. 2009; Saheb et al. 2009), demonstrating the stability of hibbingite in chloride-rich environments. Therefore, the early results from Telander and Westerman (1993 and 1997), and the more recent results from Roselle (2009, 2010, 2011a, 2011b, 2013) and Nemer et al. (2011) all indicate that the likely corrosion product is either $Fe(OH)_2$ or $Fe(II)_2(OH)_3Cl(cr)$, both of which are Fe(II) products, fixing the STOIFX parameter at a value of 1.

Section 2.3.4 of Appendix SOTERM-2014 incorrectly refers to Roselle's work and has therefore been revised as follows (provided in blue font):

> "In fact, Roselle (Roselle 2013) states that ~~green rust~~ $Fe(OH)_2$ is the most likely corrosion product in experiments with low atmospheric CO_2 concentrations ~~(<350 ppm)~~."

These changes have been added to Enclosure 4, CRA-2014 Errata Tracking.

4. Summary

The corrosion products in Roselle's experiments have not been quantitatively identified, and he found no indication that the most likely corrosion product observed by Telander and Westerman (1993), being $Fe(OH)_2$, will differ significantly from his results or that green rust, a transient product, would be the major product. The major product is $Fe(OH)_2$ or possibly its successor, $Fe(II)_2(OH)_3Cl(cr)$, as time evolves. DOE maintains that the molar ratio of hydrogen gas to iron should be 1 in the anoxic corrosion of iron in the absence of CO_2. It is therefore recommended that the parameter STOIFX not be changed from its current value.

References:

Bellot-Gurlet, L., D. Neff, S. Réguer, J. Monnier, M. Saheb, and P. Dillmann. 2009. Raman studies of corrosion layers formed on archaeological irons in various media (October). Journal of Nano Research, Vol. 8, pp. 147-156.*

Génin, J.M.R., P. Refait, G. Bourrié, M. Abdelmoula, and F. Trolard. 2001. Structure and stability of the Fe(II)–Fe(III) green rust "fougerite" mineral and its potential for reducing pollutants in soil solutions. Applied Geochemistry, 16, pp. 559–570.*

Haberman, J.H., and D.J. Frydrych. 1988. Corrosion Studies of A216 Grade WCA Steel in Hydrothermal Magnesium-Containing Brines. Materials Research Society Symposium Proceedings: Scientific Basis for Nuclear Waste Management XI (pp. 761–72). Eds. M.J. Apted and R.E. Westerman. Pittsburgh: Materials Research Society.*

Kicker, D., and C. Herrick. 2013. Parameter Summary Report for the 2014 Compliance Recertification Application (Revision 0). ERMS 560298. Sandia National Laboratories, Carlsbad, NM.

Neff, D., P. Dillmann, L. Bellot-Gurlet, and G. Beranger. 2005. Corrosion of iron archaeological artefacts in soil: characterisation of the corrosion system. Corrosion Science, 47(2), 515-535.*

Nemer, M.B., Y. Xiong, A.E. Ismail, J. Jang. 2011. Solubility of $Fe_2(OH)_3Cl$ (pure-iron end-member of hibbingite) in NaCl and Na_2SO_4 brines. Chemical Geology, Vol. 280, 1-2, Jan. 2011, pp 26-32.*

Refait, Ph., D.D. Nguyen, M. Jeannin, S. Sable, M. Langumier, and R. Sabot. 2011. Electrochemical formation of green rusts in deaerated seawater-like solutions."Electrochimica Acta, Vol. 56, pp 6481-6488.*

Refait, P., M. Abdelmoula, and J.M. Génin. 1998. Mechanisms of formation and structure of green rust one in aqueous corrosion of iron in the presence of chloride ions. Corrosion Science 40(9), 1547-1560.*

Réguer, S., P. Dillman, and F. Mirambet. 2007. Buried iron archaeological artefacts: corrosion mechanisms related to the presence of Cl-containing phases. Corrosion Science 49:2726-2744.*

Rémazeilles, C., D. Neff, F. Kergourlay, E. Foy, E. Conforto, S. Réguer, P. Refait and P. Dillmann. 2009. Mechanisms of long-term anaerobic corrosion of iron archaeological artefacts in seawater. Corrosion Science 51:2932-2041.*

* Copyrighted reference not provided in Enclosure 2.

Roselle, G.T. 2009. Iron and Lead Corrosion in WIPP-Relevant Conditions: Six Month Results. Milestone Report, October 7, 2009. ERMS 546084. Sandia National Laboratories, Carlsbad, NM.

Roselle, G.T. 2010. Iron and Lead Corrosion in WIPP-Relevant Conditions: 12 Month Results. Milestone Report, October 14, 2010. ERMS 554383. Sandia National Laboratories, Carlsbad, NM.

Roselle, G.T. 2011a. Iron and Lead Corrosion in WIPP-Relevant Conditions: 18 Month Results. Milestone report. January 5, 2011. ERMS 554715. Sandia National Laboratories, Carlsbad, NM.

Roselle, G.T. 2011b. Iron and Lead Corrosion in WIPP-Relevant Conditions: 24 Month Results. Milestone report. May 3, 2011. ERMS 555426. Sandia National Laboratories, Carlsbad, NM.

Roselle, G.T. 2013. Determination of Corrosion Rates from Iron/Lead Corrosion Experiments to be Used for Gas Generation Calculations, Rev. 1. Analysis report. January 23, 2013. ERMS 559077. Sandia National Laboratories, Carlsbad, NM.

Ruby, C., A. Géhin M. Abdelmoula, J.M.R. Génin, J.P. Jolivet. 2003. Coprecipitation of Fe(II) and Fe(III) cations in sulphated aqueous medium and formation of hydroxysulphate green rust. Solid State Sciences, 5, pp. 1055–1062.*

Saheb M., Neff D., Dillmann P., Matthiesen H., Foy D., and Bellot-Gurlet L. 2009. Materials and Corrosion, Vol. 60, p. 99-105.*

Simon, L., M. François, P Refait, G. Renaudin, M. Lelaurain, and J.M.R. Génin. 2003. Structure of the Fe(II–III) layered double hydroxysulphate green rust two from Rietveld analysis. Solid State Sciences, 5, pp. 327–334.*

Telander, M.R., and R.E. Westerman. 1993. Hydrogen Generation by Metal Corrosion in Simulated Waste Isolation Pilot Plant Environments: Progress Report for the Period November 1989 Through December 1992. SAND92-7347. ERMS 223456. Sandia National Laboratories, Albuquerque, NM.

Telander, M.R., and R.E. Westerman. 1997. Hydrogen Generation by Metal Corrosion in Simulated Waste Isolation Pilot Plant Environments. SAND96-2538. Sandia National Laboratories, Albuquerque, NM.

U.S. Department of Energy (DOE). 1996. Title 40 CFR Part 191 Compliance Certification Application for the Waste Isolation Pilot Plant (October). 21 vols. DOE/CAO 1996-2184. Carlsbad Area Office, Carlsbad, NM.

U.S. Department of Energy (DOE). 2009. Title 40 CFR Part 191 Compliance Recertification Application for the Waste Isolation Pilot Plant (March). DOE 09-2434. Carlsbad Field Office, Carlsbad, NM.

U.S. Department of Energy (DOE). 2014. Title 40 CFR Part 191 Compliance Recertification Application for the Waste Isolation Pilot Plant. DOE/WIPP 2014-3503. U.S. DOE Waste Isolation Pilot Plant, Carlsbad, NM.

Xiong, Y.-L., and Lord, A.C.S. 2008. Experimental investigations of the reaction path in the MgO–CO_2–H_2O system in solutions with various ionic strengths, and their applications to nuclear waste isolation. Applied Geochemistry, 23:1634–1659.*

* Copyrighted reference not provided in Enclosure 2.

Addendums to DOE Responses to EPA Completeness Questions on the CRA-2014

In a technical exchange meeting in Albuquerque, New Mexico held February 2 and 3, 2016, the DOE and the EPA discussed DOE's responses to EPA Completeness questions on the CRA-2014 that have been submitted to date. During the technical exchange meeting, the DOE agreed to issue an addendum to 1-23-12, WIPP-Specific Organic Complexation Data, and 2-C-6, MgO Hydration Rate. On February 26, 2016, the EPA issued a letter clarifying its original comment 2-C-4, Hydromagnesite Conversion Rate, and withdrew two FEP-related comments, 2-32-S16 and 2-32-S17. In response, the DOE is submitting three addendums, 1-23-12, 2-C-4, and 2-C-6, as provided in the following text.

EPA Comment
1-23-12 WIPP-Specific Organic Complexation Data.

Appendix SOTERM Section 3.8.2 provides a description and four graphs (Figure SOTERM-21) that relate to WIPP-specific experiments designed to evaluate the effects of organic chelating agents on +III and +IV actinide solubility in WIPP brines.

1. *Please provide supporting documentation for these data, including a summary of the experimental approach, materials and analytical methods used to produce the data.*
2. *Please provide any available characterization data for the solid phases present in these experiments.*

DOE Response

In the technical exchange meeting between DOE and EPA in Albuquerque, New Mexico, held February 2 and 3, 2016, the DOE agreed to submit an addendum to the original response that provides more information on the Th(IV) organic-effects data. The data reported in Appendix SOTERM-2014 on the effects of organics on the solubility of the An(III) and An(IV) actinides are initial data as this remains an ongoing area of investigation for the WIPP.

The Th(IV) results briefly discussed in the text of Appendix SOTERM-2014, Section 3.8.2, were performed according to the following procedure:

- GWB brine at $pC_{H+} \sim 9$ was prepared according to established procedures. Fifteen mL of this brine was placed in 30 mL polypropylene bottles.
- Acetate, oxalate, citrate and EDTA were added (as sodium salts), leading to their dissolution in the GWB brine to the approximate concentrations calculated based on the masses reported in the CRA-2009 inventory report [Leigh, Trone, and Fox 2005]. These were measured to be 2.4 mM, 30 mM, 3.9 mM and 0.09 mM for acetate, oxalate, citrate and EDTA, respectively, using a Dionex DX-500 ion chromatograph.
- After two days of equilibration, ~ 0.1 g of thorium, as a thorium nitrate hydrate salt, was added to the brine. This led to rapid dissolution, complexation (if any) with the organics, and re-precipitation as a thorium oxyhydroxide amorphous phase. The thorium concentration was determined by ICP-MS after 20 nm ultrafiltration. No follow-up solid characterizations were performed on the thorium precipitates since phase alteration was not expected and the initial phase was amorphous.
- Replicate experiments were performed at room temperature (21 ± 3 °C) and in the dark to minimize light-induced organic degradation.
- Periodic samples were taken over a relatively short time (a few weeks) to confirm the stability of the organics added and determine the concentration of thorium in solution.

As reported, the final thorium concentration at $pC_{H+} = 9.3$ was in agreement with the organic-free solubility studies when no carbonate was present. This low impact of organics on the solubility of thorium is a preliminary observation based on data obtained through the CRA-2014 cutoff date.

References:

Leigh, C., J. Trone, and B. Fox. 2005. TRU Waste Inventory for the 2004 Compliance Recertification Application Performance Assessment Baseline Calculation (Revision 0). ERMS 541118. Sandia National Laboratories, Carlsbad, NM.

EPA Comment

1. Addendum to Comment 2-C-4 (a)

In completeness comment 2-C-4, EPA stated that DOE must re-evaluate the rate of hydromagnesite conversion to magnesite that was used in the CRA 2014 PA (Edwards 2015). DOE's response to this comment (Franco 2015) indicates that there was confusion about the meaning of this comment. Comment 2-C-4 is reworded as follows to provide clarification:

2-C-4 Hydromagnesite Conversion Rate. *Clayton (2013) formulated the conversion reaction from hydromagnesite to magnesite for inclusion in the BRAGFLO calculations as:*

$$Mg_5(CO_3)_4(OH)_2 \cdot 4H_2O(s) \rightarrow 4\ MgCO_3(s) + Mg(OH)_2(s) + 4\ H_2O(l) \qquad (5)$$

*Clayton (2013) calculated a range for the hydromagnesite conversion rate based on assumed reaction times of 100 to 10,000 years (Cases A and B, Table 1), citing the EPA (1998) evaluation of hydromagnesite conversion times of "hundreds to perhaps thousands of years.". However, Clayton (2013) did not consider an updated evaluation of hydromagnesite conversion times (SCA 2008). SCA (2008) reviewed the available experimental and natural analogue data and concluded that it was possible that no hydromagnesite would convert to magnesite over the 10,000 year period of performance (Case C). Consequently, the available data show that the lower limit of the reaction rate distribution should be 0 mol/kg*s (Case C).*

Table 1. Effects of Reaction Times on Hydromagnesite Conversion Reaction Rates and Hydromagnesite Remaining after 10,000 Years

Description	Reaction Time (years)	Reaction Rate (mol/kg*s)	Hydromagnesite After 10,000 Years (%)
Case A: Clayton (2013) maximum rate	100	6.8×10^{-10}	0
Case B: Clayton (2013) minimum rate	10,000	6.8×10^{-12}	0
Case C: SCA (2008) minimum rate	Infinite	0	100

*Clayton (2013) cited a minimum reaction time (maximum reaction rate) of "hundred" of years based on EPA (1998), but then used a shorter minimum reaction time of 100 years to calculate the maximum reaction rate without providing adequate justification. The minimum 100 year reaction time is inconsistent with the available reaction rate data. For example, Zhang et al. (2000) extrapolated higher-temperature experimental rate data obtained in GWB brine to 25°C and determined an induction period of 200 years and a reaction half-time of 73 years. This extrapolated rate is consistent with a higher minimum reaction time (on the order of 350 years), which would result in a lower maximum reaction rate than the 6.8×10^{-10} mol/kg*s maximum rate used by Clayton (2013).*

*The effect of using 0 mol/kg*s (Case C) rather than 6.8×10^{-12} mol/kg*s (Case B) as the minimum conversion rate is likely to be less brine production in the water balance. DOE should use 0 mol/kg*s as the lower limit of the hydromagnesite conversion rate. DOE should also re-evaluate the upper limit of the hydromagnesite conversion rate, select a lower maximum conversion rate (minimum reaction time greater than 100 years) that is consistent with the available data and provide adequate justification for the maximum conversion rate.*

References:

Clayton, D.J. Justification of Chemistry Parameters for Use in BRAGFLO for AP-164, Rev. 1. Sandia National Laboratories, ERMS 559466.

Edwards, J.D. 2015. Second Set of CRA 2014 Completeness Comments. U.S. Environmental Protection Agency Letter to J.R. Franco, U.S. Department of Energy, February 27, 2015.

EPA (U.S. Environmental Protection Agency). 1998. Technical Support Document for Section 194.24: EPA's Evaluation of DOE's Actinide Source Term. Environmental Protection Agency Office of Radiation and Indoor Air, Washington, DC. Docket A-93-02, Item V-B-17.

Franco, J.R. 2015. Response to Environmental Protection Agency Letters Dated December 7, 2014 and February 27, 2015 Regarding the 2014 Compliance Recertification Application. U.S. Department of Energy, Carlsbad Field Office, May 29, 2015.

SCA (S. Cohen and Associates). 2008. Review of MgO-Related Uncertainties in the Waste Isolation Pilot Plant. Final Report prepared for the U.S. Environmental Protection Agency Office of Radiation and Indoor Air. January 24, 2008.

Zhang, P.C, H.L. Anderson, J.W. Kelly, J.L. Krumhansl and H.W. Papenguth. 2000. Kinetics and Mechanisms of Formation of Magnesite from Hydromagnesite in Brine. Sandia National Laboratories, SAND99-1946J, ERMS 514868.

DOE Response

This addendum to DOE's response to EPA Comment 2-C-4 evaluates data from *Kinetics and Mechanisms of Formation of Magnesite from Hydromagnesite in Brine* (Zhang et al. 2000) that are relevant to determining an appropriate range of times and rates for the conversion of hydromagnesite to magnesite in the WIPP repository environment. S. Cohen and Associates (SCA) discuss other sources of data in the *Review of MgO-Related Uncertainties in the Waste Isolation Pilot Plant* (SCA 2008), but those data do not appear to be conclusive regarding conversion rates and disagree with the WIPP-specific experiments conduct by Zhang et al. (2000). Specifically, the brines that will be present in the repository under the disturbed scenarios. In the playa basins of the Cariboo Plateau in British Columbia, sedimentary magnesite and hydromagnesite of Holocene age are observed (Renaut and Stead 1990). Of note, "magnesite and hydromagnesite are forming today at Milk Lake and in many other playa basins on the Cariboo Plateau" (Renaut and Stead 1990). Therefore, the wide range of conversion times (i.e., 6,000 years to 30,000,000) mentioned by SCA (2008), especially, the high end conversion times, might be applicable to the situations where the presence of brines is absent or intermittent, but is not applicable to the WIPP where the repository is in equilibrium with the brines. Hence they were not used in the evaluation. The reaction time range of 100 to 10,000 years used in the derivation of hydromagnesite to magnesite conversion rates from Clayton (2013) was based on a "round number" estimate from the EPA (1998) report, with the values chosen to ensure that the entire range was encompassed. In evaluating the data presented in SCA (2008) (specifically, the Zhang et al. (2000) data), we have derived a reaction time range based on WIPP specific data (Table 4).

The Zhang et al. (2000) data do not support the EPA's request to lower the reaction rate to zero (i.e., specifying an infinite reaction time). While the Zhang et al. (2000) report did show that reaction half time of up to 30,000,000 years could be calculated assuming a fourth-order kinetic equation, that same report rejected the use of that equation. Furthermore, the current evaluation does not support a minimum reaction time greater than 100 years; instead, a lower bound on reaction time of 18 years (Table 4) is

reasonable based on the available data. Although the DOE was requested by the EPA to increase the reaction time (decrease maximum rate), we were also asked to "re-evaluate the upper limit of the hydromagnesite conversion rate." The analysis of the Zhang et al. (2000) data suggests a smaller reaction time is reasonable and the analysis is given below.

The SCA (2008) report concluded, in part, the following:

> *Based on the information reviewed above, there is significant uncertainty regarding the rate at which hydromagnesite can convert to magnesite, and whether all hydromagnesite will convert to magnesite during the WIPP regulatory time period. There are many uncertainties associated with the extrapolation of the Zhang et al. (2000) laboratory data to WIPP conditions, including the form of the rate equation, the effects of the hydromagnesite chemical and physical properties on the induction period, the uncertainties in determining the rates during the induction period, and whether the activation energy will remain constant at lower temperatures.*

The SCA (2008) report also points out that the Zhang et al. (2000) study reported "order-of-magnitude uncertainties associated with the induction period calculations."

The Zhang et al. (2000) study cited in the SCA (2008) report extrapolated high temperature (110-200 °C) experimental reaction rates to lower temperature (25 °C) conditions. In Zhang et al. (2000), reaction half times, which are the times for transformation of 50% of hydromagnesite(5424) [$Mg_5(CO_3)_4(OH)_2 \cdot 4H_2O$] to magnesite ($MgCO_3$), were found to depend on the chemistry of the supporting solutions. In saturated NaCl solution, which is chemically similar to the WIPP brine ERDA-6, the mean calculated reaction half-time at 25 °C is 4.7 years. In the solution denoted as GW brine, which is chemically similar to the WIPP brine GWB, the mean calculated reaction half-time at 25 °C is 73 years. In Zhang et al. (2000), the induction periods, which are defined as an interval of minimal transformation, were extrapolated to 25 °C, giving values of 18 years for the ERDA-6 equivalent brine and 200 years for the GWB equivalent brine, again reflecting the influence of the chemistry of the supporting solutions on the hydromagnesite to magnesite conversion.

Because of the high level of uncertainty in the reaction rates, as well as the substantial dependence on the chemistry of the supporting solutions, the upper and lower bounds of the reaction rate should encompass these uncertainties. As discussed in Zhang et al. (2000), the induction period accounts for the conversion of the first ~5%. Since the study reported "order-of-magnitude uncertainties associated with the induction period calculations," assume that the lower bound of the induction time is one tenth the upper bound of induction time and the mean induction time is the mean of the upper and lower bounds. In mathematical terms:

$$IT_{mean} = \frac{IT_{lb} + IT_{ub}}{2}, \tag{1}$$

and

$$IT_{ub} = 10(IT_{lb}), \tag{2}$$

where IT_{mean} is the mean induction time and subscripts *lb* and *ub* denote lower and upper bounds, respectively. Substituting equation (2) into equation (1) and solving for the lower and upper bounds gives:

$$IT_{lb} = 0.182 \times IT_{mean}, \tag{3}$$

and $$IT_{ub} = 1.82 \times IT_{mean}. \quad (4)$$

The lower bound induction time is the mean induction time multiplied by 0.182 and the upper bound induction time is the mean induction time multiplied by 1.82. The calculated induction times using equations (3) and (4) are shown in Table 1 for the WIPP equivalent brines.

Table 1. Mean, lower and upper bounds for the hydromagnesite to magnesite induction time for the two equivalent WIPP brines.

Brine	Mean Induction Time [yr]	Induction Time Upper Bound [yr]	Induction Time Lower Bound [yr]
GWB Equivalent	200	364	36
ERDA-6 Equivalent	18	33	3.3

The reaction rate for the remaining 95% hydromagnesite mass is given by Zhang et al. (2000) as:

$$\frac{M}{M_0} = e^{-kt}, \quad (5)$$

or $$\ln(M / M_0) = -kt, \quad (6)$$

where M is the mass of hydromagnesite, M_0 is the initial mass of hydromagnesite, k is the reaction rate, and t is time. Zhang et al. (2000) report the mean calculated rates at 25 °C, along with the calculated standard deviations for both brines in Table 4 of their report. These values are reproduced below in Table 2. For this analysis, the upper bound of the reaction rate is assumed to be the mean rate plus one standard deviation, while the lower bound of the reaction rate is assumed to be the mean rate minus one standard deviation. These upper and lower bounds of the values of k are also shown in Table 2.

Table 2. Mean, standard deviation, lower and upper bounds for the hydromagnesite to magnesite reaction rate for the two equivalent WIPP brines.

Brine	Mean Reaction Rate [hr^{-1}][a]	Standard Deviation [hr^{-1}][a]	Reaction Rate Lower Bound [hr^{-1}]	Reaction Rate Upper Bound [hr^{-1}]
GWB Equivalent	1.085×10^{-6}	6.656×10^{-7}	4.194×10^{-7}	1.751×10^{-6}
ERDA-6 Equivalent	1.699×10^{-5}	5.727×10^{-6}	1.126×10^{-5}	2.272×10^{-5}

[a] From Table 4 of Zhang et al. (2000).

The total reaction time can then be calculated as the sum of the induction time for ~5% of the hydromagnesite mass to convert to magnesite (shown in Table 1) and the time for the remaining 95% hydromagnesite mass to convert to magnesite based on the reaction rates in Table 2. The time for 95% conversion, T, is based on equation (6):

$$T = \frac{-\ln(M / M_0)}{k} = \frac{-\ln(0.05)}{k} \quad (7)$$

where M/M_0 is replaced by 0.05 for the remaining 95% to react and the value of k is a lower bound or upper bound for the reaction rate in Table 2. The calculated values of T, based on equation (7) and converted from hours to years (8766 hour/year), are shown in Table 3.

Table 3. Lower and upper bounds for the calculated reaction times of the remaining 95% hydromagnesite to magnesite conversion for the two equivalent WIPP brines.

Brine	Mean Reaction Time [yr]	Reaction Time Upper Bound [yr]	Reaction Time Lower Bound [yr]
GWB Equivalent	315	815	195
ERDA-6 Equivalent	20.1	30.4	15.0

Table 4 shows the result of summing the times for the induction period (Table 1) and the remaining 95% conversion time (Table 3) to get an overall conversion time. Table 5 shows the corresponding reaction rates, which are calculated by taking the inverse of the reaction times (in seconds) and dividing by the hydromagnesite molecular weight (0.468 kg/mol). The resultant rate in mol(hydromagnesite)/kg(hydromagnesite)/s is in the appropriate units for use in the BRAGFLO code (Clayton 2013).

Table 4. Lower and upper bounds for the overall hydromagnesite conversion times for the two equivalent WIPP brines.

Brine	Mean Reaction Time [yr]	Reaction Time Upper Bound [yr]	Reaction Time Lower Bound [yr]
GWB Equivalent	515	1,180	232
ERDA-6 Equivalent	38	63	18

Table 5. Lower and upper bounds for the overall calculated reaction rates for the hydromagnesite to magnesite conversion for the two equivalent WIPP brines.

Brine	Mean Reaction Rate [mol/kg/s]	Reaction Rate Lower Bound [mol/kg/s]	Reaction Rate Upper Bound [mol/kg/s]
GWB Equivalent	1.3×10^{-10}	5.7×10^{-11}	2.9×10^{-10}
ERDA-6 Equivalent	1.8×10^{-9}	1.1×10^{-9}	3.7×10^{-9}

We agree that there are uncertainties in the results from Zhang et al. (2000) and have tried to incorporate an appropriate level of uncertainty into the calculated values for the induction period and the 95% conversion time, accounting for the substantial dependence on the chemistry of the supporting solutions.

This evaluation of the Zhang et al. (2000) report supports a distribution of hydromagnesite conversion rates from 5.7×10^{-11} mol/kg/s to 3.7×10^{-9} mol/kg/s (see Table 5).

The amount of water available to the repository due to the conversion of hydromagnesite to magnesite would be modified by changing the distribution of hydromagnesite conversion rates. The potential effects on performance assessment of changing the bounds of the reaction rate can be estimated by examining the impact of the sampled hydromagnesite conversion rate on the final output. In the *Sensitivity of the CRA-2014 Performance Assessment Releases to Parameters* (Kirchner 2013), Kirchner documents the sensitivity of releases to sampled input parameters. The parameter used to represent the hydromagnesite conversion rate (WAS_AREA:HYMAGCON) had a distribution corresponding to a conversion time of 100 to 10,000 years, and did not show any correlation with releases from the repository. Therefore, the potential effects on performance assessment of changing the sampled bounds for the hydromagnesite conversion rates to the range in Table 5 are expected to be minimal because the majority of the range of the calculated conversion times, 18 to 1,180 years (see Table 4), is between 100 to 10,000 years. Based on this analysis and the uncertainty, DOE recommends changing the maximum reaction rate to 3.7×10^{-9} mol/kg/s (18 year conversion time) and keeping the same lower bound of reaction rate (10,000 year conversion time) as was used in the CRA-2014. These values ensure that the entire range observed in the Zhang et al. data is encompassed.

References:

Clayton, D. 2013. Justification of Chemistry Parameters for Use in BRAGFLO for AP-164, Rev. 1. ERMS 559466. Sandia National Laboratories, Carlsbad, NM.

Kirchner, T. 2013. Sensitivity of the CRA-2014 Performance Assessment Releases to Parameters. ERMS 560043. Sandia National Laboratories, Carlsbad, NM.

Renault, R.W. and Stead, D., 1990. Recent Magnesite-Hydromagnesite Sedimentation in Playa Basins of the Cariboo Plateau, British Columbia (92P). *BC Ministry of Energy, Mines and Petroleum Resources*, pp.1991-1.*

SCA (S. Cohen and Associates). 2008. Review of MgO-Related Uncertainties in the Waste Isolation Pilot Plant. Final Report prepared for the U.S. Environmental Protection Agency Office of Radiation and Indoor Air, Washington, D.C., January 24, 2008.

U.S. Environmental Protection Agency (EPA). 1998. Technical Support Document for Section 194.24: EPA's Evaluation of DOE's Actinide Source Term. Docket A-93-02, Item V-B-17. Environmental Protection Agency Office of Radiation and Indoor Air, Washington, D.C.

Zhang, P.C., H.L. Anderson, J.W. Kelly, J.L. Krumhansl and H.W. Papenguth. 2000. Kinetics and Mechanisms of Formation of Magnesite from Hydromagnesite in Brine. SAND99-1946J. ERMS 514868. Sandia National Laboratories.*

* Copyrighted reference not provided in Enclosure 2.

EPA Comment

2-C-6 MgO Hydration Rate. *MgO has been supplied for the WIPP engineered barrier by three vendors: National Magnesia Chemicals, Premier Chemicals, and, currently, from Martin Marietta Magnesia Specialties (Martin Marietta). The majority of the MgO in the repository is from Premier Chemicals and Martin Marietta. Clayton (2013) used MgO hydration rates obtained from experiments conducted with MgO supplied by Premier Chemicals to establish the hydration rates used in PA. However, Wall (2005) performed preliminary tests with the Martin Marietta MgO and concluded that it reacted to form brucite faster than Premier MgO. Given the multiple vendors that supply MgO a summary of the following information needs to be provided;*

- *The inundated and humid MgO hydration rates for MgO from the three vendors.*
- *The potential effects of the variable MgO hydration rates on repository performance.*
- *The amounts of National Magnesia Chemicals, Premier MgO and Martin Marietta MgO that will be present in the WIPP repository at the time of closure, and assumptions regarding the future source(s) of MgO.*

References:

Clayton, D.J. 2013. Justification of Chemistry Parameters for Use in BRAGFLO for AP-164, Rev. 1. Sandia National Laboratories, ERMS 559466.

Deng, H., M. Nemer, and Y. Xiong. 2007. Experimental Study of MgO Reaction Pathways and Kinetics Rev. 1. Sandia National Laboratories TP 06-03.

Deng, H., Y. Xiong, M. Nemer and S. Johnsen. 2009. Experimental Work Conducted on MgO Long-Term Hydration. Sandia National Laboratories ERMS 551421.

Wall, N.A. 2005. Preliminary Results for the Evaluation of Potential New MgO. Sandia National Laboratories ERMS 538514.

DOE Response

In the technical exchange meeting between DOE and EPA at Albuquerque, New Mexico, February 2 through 3, 2016, DOE agreed to provide an addendum to the EPA's completeness comment 2-C-6. The following is an addendum to the DOE's original response to the EPA's completeness comment 2-C-6, submitted to the EPA on May 29, 2015.

At the data cut-off date for CRA-2014, the hydration rates for MgO from Martin Marietta Magnesia Specialties were not processed into the form that was usable for the Performance Assessment (PA). When the data are processed into the form that is usable for PA, the hydration rates for Martin Marietta will be combined with the hydration rates for Premier MgO to be used for PA in a fashion (e.g., weighted averages) that accounts for their respective contributions to the total MgO inventory in the repository. As the contribution from MgO of National Magnesia Chemicals is less than 0.5%, its hydration rates will not be considered in the future calculations.

Status Report of DOE Responses to EPA Completeness Questions				
Completeness Question	**Included in This Submittal**	**Previously Submitted**	**Pending**	**Withdrawn by the EPA**
EPA's Completeness Questions Received December 17, 2014				
40 CFR 194.15(A)(2) MONITORING **1-15-1 Water Level Fluctuations in SNL-13.** DOE/WIPP-12-3489 p. 143 states "SNL-13 was also excluded [from the Culebra groundwater analysis] due to a sudden rise and then sudden stabilization following the drilling of a new oil or gas well nearby." Please address		✓		
40 CFR 194.15(A)(2) MONITORING **1-15-2 Shaft Extensometers Not Taking Recordings.** DOE is not replacing the failed monitoring instruments in the shaft. However, EPA Section 42, Monitoring requirements expects, " *...extent of deformation ..." and "...brittle deformation...* " to be monitored. Please		✓		
40 CFR 194.15(A)(2) MONITORING **1-15-3 Derivation of Annual Culebra Water Level Map.** CRA-2014 Section 42.8 *Changes or New Information Since the CRA-2009* discusses changes to the process used to derive the Culebra groundwater flow parameters that is used to prepare the annual water level map.		✓		
40 CFR 194.23 MODELS AND COMPUTER CODES **1-23-1 Continuing Validity of Kds.** CRA-2014 Appendix PA, Table PA-1 states that the Culebra Matrix Partition Coefficients (Kds) are, " *Carried over from CRA-2009 PABC* ." Please provide the rationale for the assumption that the CRA 2014 Kds can be		✓		
40 CFR 194.23 MODELS AND COMPUTER CODES **1-23-2 Continuing Validity of T-Fields.** CRA-2014 Appendix PA, Table PA-1 states that the Culebra Transmissivity Fields are, " *Carried over from CRA-2009 PABC* ." It appears that the last update to the geologic well data analysis was performed in 2007 (Powers		✓		
40 CFR 194.23 MODELS AND COMPUTER CODES **1-23-3 REGION ROMPCS** The Agency agreed to the adopted parameter values used for the panel closure change request to isolate the effects and facilitate a comparison of the proposed panel closure design on the baseline PA and, at the time of		✓		
40 CFR 194.23 MODELS AND COMPUTER CODES **1-23-4 REGION DRZ PCS** The Agency would like DOE to address the following comments related to the parameter values adopted for the DRZ_PCS:		✓		
40 CFR 194.23 MODELS AND COMPUTER CODES **1-23-5 Waste Shear Strength.** Please address the following: 1. Provide horsetail plots of the remaining fraction of uncorroded iron in the repository throughout the 10,000-		✓		

Status Report of DOE Responses to EPA Completeness Questions				
Completeness Question	**Included in This Submittal**	**Previously Submitted**	**Pending**	**Withdrawn by the EPA**
40 CFR 194.23 MODELS AND COMPUTER CODES **1-23-6 Probability of Encountering a Castile Brine Pocket.** Please address the following comments: 1. TDEM results are site specific and indicate the presence of potentially large volumes of brine beneath some		✓		
40 CFR 194.23 MODELS AND COMPUTER CODES **1-23-7. Volume of Repository Operations and Experimental Areas.** Please address the following: 1. Explain how DOE arrived at a volume of 148,011 m^3 for the underground.		✓		
40 CFR 194.23 MODELS AND COMPUTER CODES **1-23-8 Fluid Flow in Repository Operations and Experimental Areas.** There have been numerous refinements of conceptual and numerical models of repository fluid flow since the 1994-95 time frame as well as changes to the panel closure system that may also change repository fluid flow.		✓		
40 CFR 194.23 MODELS AND COMPUTER CODES **1-23-11 EQ3/6 and Supporting Files.** Please provide the following computer files related to the actinide source term modeling calculations and the determination of the cumulative distribution functions for the actinide solubilities:		✓		
40 CFR 194.23 MODELS AND COMPUTER CODES **1-23-12 WIPP-Specific Organic Complexation Data.** Appendix SOTERM Section 3.8.2 provides a description and four graphs (Figure SOTERM-21) that relate to WIPP-specific experiments designed to evaluate the effects of organic chelating agents on +III and +IV actinide		✓		
40 CFR 194.23 MODELS AND COMPUTER CODES **1-23-13 Missing Reference.** Appendix SOTERM, Figure SOTERM-7 caption cites Altmaier (2011) but this reference is missing from the reference list. Please provide this reference.		✓		
40 CFR 194.24 WASTE CHARACTERIZATION- PERFORMANCE ASSESSMENT INVENTORY **1-24-1 Shielded Container Lead Inventory** 1. Please provide information as to how lead shielding on RH shielded containers is included in the performance assessment.		✓		
40 CFR 194.24 WASTE CHARACTER IZATION- PERFORMANCE ASSESSMENT INVENTORY **1-24-2 Inventory Report Text Unclear.** Please address the following: 1. Provide information as to how the "projected-to-stored volume ratio" is derived for both RH and CH waste.		✓		

Status Report of DOE Responses to EPA Completeness Questions				
Completeness Question	**Included in This Submittal**	**Previously Submitted**	**Pending**	**Withdrawn by the EPA**
40 CFR 194.24 WASTE CHARACTER IZATION- PERFORMANCE ASSESSMENT INVENTORY **1-24-3 Emplaced Inventory Chemical Constituents** 1. In the ATWIR 2012, Section 2.3, it is stated that, "Chemical constituents are not reported in the emplaced inventory". In the PAIR 2012 report, Section 4.3, it is indicated that "two additional analysis" were performed for		✓		
40 CFR 194.24 WASTE CHARACTER IZATION- PERFORMANCE ASSESSMENT INVENTORY **1-24-4 Missing References.** Please provide the following references: French, D. 2009. *Analysis of Container Material Masses* , INV-SAR-19. Los Alamos National Laboratory -		✓		
GENERAL: CRA-2014 DOCUMENTATION **1-G-1 Reference Appendix QAPD-2014 Not Provided.** CRA-2014 Section 23, Models and Computer Codes, Section 23.5.7 states, "The DOE's quality assurance program, as applied to the CRA-2014, is contained in Appendix QAPD-2014." The appendix has not been		✓		
GENERAL: CRA-2014 DOCUMENTATION **1-G-2 Codes IDs Do Not Include Source Code Listing.** CRA-2014 Section 23, Models and Computer Codes, Section 23.8.7 states, "The IDs include source-code listings..." EPA examined a number of code Implementation Documents; they include a reference to the		✓		
GENERAL: CRA-2014 DOCUMENTATION **1-G-3 New Codes EQ3/6 and JAS3D Documentation Incomplete.** DOE states in CRA-2014 Section 23, 23.7.7, "The documentation for the new codes EQ3/6 and JAS3D may be found in their respective UM, AP, VD, ID, and RD/VVP." It does not appear that this documentation has been		✓		
CHEMISTRY COMMENTS **1-C-1 LANL Waste Stream With Added Cellulosic Material.** Organic kitty litter was used as an absorbent for nitrate salts for Waste Stream LA-MIN02-V.001 (NMED 2014) and 349 drums of this waste were placed in Panels 6 and 7 (Wallace 2014). Please address the following:		✓		
EPA's Completeness Questions Received February 27, 2015				
194.23 MODELS AND COMPUTER CODES **2-23-1 ROM Salt Panel Closures Locations.** Please provide the WIPP configuration layout (a plan view) used for the 2014 CRA that includes all locations where the ROM salt panel closures are to be placed. Provide text that provides the exact location, dimensions		✓		
194.23 MODELS AND COMPUTER CODES **2-23-2 Provide An Update of the Derivation of the Shaft Properties at the Repository Horizon.** In the BRAGFLO grid for the 2004 and 2009 CRA Performance Assessments (PAs), the modeled lower portion of the shaft included an effective permeability that incorporated both the concrete portion of the shaft (at the		✓		

Status Report of DOE Responses to EPA Completeness Questions				
Completeness Question	**Included in This Submittal**	**Previously Submitted**	**Pending**	**Withdrawn by the EPA**
194.33 FUTURE DRILLING **2-33-1 Future Drilling Into Nitrate Waste.** Please provide the probability and describe the potential consequence(s) to PA calculations of drilling into the nitrate waste.		✓		
194.43 PASSIVE INSTITUTIONAL CONTROLS **2-43-1 Changes in Passive Institutional Controls (PICs).** Recent Nuclear Energy Agency and International Atomic Energy Agency reports describe changes and developments in international approaches to PICs. These are referenced in INIS-US-13-WM-13145 which		✓		
194.44 ENGINEERED BARRIERS **2-44-1 MgO Physical Segregation.** In Franco (2012) DOE notified EPA that MgO emplacement has been modified by placing a 3,000 pound supersack of MgO on every other waste stack or on each waste stack in every other row. In the Franco 2012		✓		
194.46 REMOVAL OF WASTE **2-46-1 CCA Appendix WRAC Waste Removal Documentation Needs Updating.** The cited removal plan is basically the same as that given during the 1996 CCA and does not reflect updates and modifications to the repository design and waste characteristics. The Agency found discrepancies between		✓		
194.55 RESULTS OF COMPLIANCE ASSESSMENTS **2-55-1 Incorrect Reference.** Appendix IGP-2014, Section IGP-2.1 makes reference to 194.55(b)(1), should this be 194.54(b)(1) "Existing boreholes..."?		✓		
CHEMISTRY COMMENTS **2-C-3 Data Supporting Water Balance Assumptions.** The CRA-2014 PA calculations include the effects of MgO hydration, microbial degradation of CPR and iron sulfide formation on repository water balance. For PA, it is assumed that hydrogen sulfide created by CPR		✓		
CHEMISTRY COMMENTS **2-C-4 Hydromagnesite Conversion Rate.** Clayton (2013) formulated the conversion reaction from hydromagnesite to magnesite for inclusion in the BRAGFLO calculations as:$Mg5(CO3)4(OH)2{\bullet}4H2O(s) \rightarrow 4\ MgCO3(s) + Mg(OH)2(s) + 4\ H2O(l)$ (5) Clayton		✓		
CHEMISTRY COMMENTS **2-C-5 Cumulative Effects of Water Balance Assumptions on PA.** The result of several water balance assumptions is to increase brine production from waste reactions in the repository. These assumptions include that hydrogen sulfide will preferentially react with iron hydroxide instead		✓		

Status Report of DOE Responses to EPA Completeness Questions				
Completeness Question	**Included in This Submittal**	**Previously Submitted**	**Pending**	**Withdrawn by the EPA**
CHEMISTRY COMMENTS **2-C-6 MgO Hydration Rate.** MgO has been supplied for the WIPP engineered barrier by three vendors: National Magnesia Chemicals, Premier Chemicals, and, currently, from Martin Marietta Magnesia Specialties (Martin Marietta). The majority of		✓		
CHEMISTRY COMMENTS **2-C-7 MgO Hydration Rate Data File.** Please provide a copy of the Microsoft Excel file "hydration kinetics Q & HY2 & HH djc 5-1-07.xls" used by Nowak and Clayton (2007) to calculate the MgO hydration rates. References: Nowak, E.J. and D. Clayton.		✓		
CHEMISTRY COMMENTS **2-C-8 Iron and Lead Corrosion Rate Data.** Please provide spreadsheets containing the iron and lead corrosion data listed in Appendix A, Tables A-1 and A-2 from Roselle (2013). References: Roselle, G.T. 2013. Determination of Corrosion Rates from Iron/Lead		✓		
194.32 SCOPE OF PERFORMANCE ASSESSMENT Since the original certification decision changes have been made to the repository, it is our observation that, for many of the features, events, and processes (FEPs) we have reviewed, DOE has not fully considered all of the relevant changes to the repository. Additionally, DOE has not fully considered updates relevant to activities		✓		
194.32 SCOPE OF PERFORMANCE ASSESSMENT **2-32-S1.** Screening argument considers only boreholes intersecting the waste region. Please supplement the argument with a discussion of boreholes that intersect the non-waste regions and the consequence to PA calculations.		✓		
194.32 SCOPE OF PERFORMANCE ASSESSMENT **2-32-S2.** The screening argument considers flow into the repository from boreholes that intercept pressurized fluid in underlying formations but only for boreholes intersecting the waste region. In the current BRAGLO model gas		✓		
194.32 SCOPE OF PERFORMANCE ASSESSMENT **2-32-S3.** Screening argument considers only boreholes intersecting the waste region and also pressurized Castile brine. In the current BRAGLO model gas and brine readily flow between the waste and non-waste regions. Please		✓		
194.32 SCOPE OF PERFORMANCE ASSESSMENT **2-32-S4.** Please address whether enhanced production techniques are being used in the Delaware basin and in the vicinity of WIPP. Please also address the potential for these techniques to create a preferential pathway for		✓		

Status Report of DOE Responses to EPA Completeness Questions				
Completeness Question	**Included in This Submittal**	**Previously Submitted**	**Pending**	**Withdrawn by the EPA**
194.32 SCOPE OF PERFORMANCE ASSESSMENT **2-32-S5.** This FEP is screened out partially on the basis that solution mining will not occur in low ambient temperature conditions. However, solution mining is occurring in the nearby Eddy mine under similar conditions that exist in		✓		
194.32 SCOPE OF PERFORMANCE ASSESSMENT **2-32-S6**. In the screening argument please provide evidence that the modeled excavated volume is the expected mined volume of the underground workings at the time of closure.		✓		
194.32 SCOPE OF PERFORMANCE ASSESSMENT **2-32-S7.** The screening argument citation of the CCA as the source of information on the Heterogeneity of waste forms ignores changes that have occurred in the past 15 years, including supercompacted waste and mingling RH		✓		
194.32 SCOPE OF PERFORMANCE ASSESSMENT **2-32-S8.** Please supplement the screening argument with an explanation of the implementation in PA of the material inventory of shielded containers containing RH waste.		✓		
194.32 SCOPE OF PERFORMANCE ASSESSMENT **2-32-S9**. The screening argument for this FEP states "This excavation-induced, host-rock fracturing is accounted for in PA calculations (the CCA, Chapter 6.0, Section 6.4.5.3)." The cited CCA text indicates that the DRZ is modeled		✓		
194.32 SCOPE OF PERFORMANCE ASSESSMENT **2-32-S10.** Screening argument was combined with that for W18 *Disturbed Rock Zone(DRZ); please see comments for FEP W18.*		✓		
194.32 SCOPE OF PERFORMANCE ASSESSMENT **2-32-S11.** Please supplement the screening argument with a discussion of salt creep and consolidation specific to the ROM salt in the ROMPCS, and healing of the adjacent DRZ. Such a discussion can be found in Camphouse et		✓		
194.32 SCOPE OF PERFORMANCE ASSESSMENT **2-32-S12.** Screening argument was combined with that for W20 *Salt Creep* ; please see comments for FEP W20. Additionally, please supplement the screening argument with discussions of 1) the coupling between		✓		

Status Report of DOE Responses to EPA Completeness Questions				
Completeness Question	**Included in This Submittal**	**Previously Submitted**	**Pending**	**Withdrawn by the EPA**
194.32 SCOPE OF PERFORMANCE ASSESSMENT **2-32-S13**. Please supplement the screening argument with a discussion of the potential for high waste panel gas pressures to delay the consolidation of the ROM salt, thereby maintaining a higher permeability in the PCS for a		✓		
194.32 SCOPE OF PERFORMANCE ASSESSMENT **2-32-S14.** Please update the screening argument to reflect the LANL inventory with nitrates and added organic matter that resulted in an exothermic reaction.		✓		
194.32 SCOPE OF PERFORMANCE ASSESSMENT **2-32-S15**. Please modify the screening argument to address whether, in addition to "a reduction of TRU radionuclides from previous estimates", the quantities of fissile radionuclides have also been reduced.		✓		
194.32 SCOPE OF PERFORMANCE ASSESSMENT **2-32-S16**. Please supplement the screening argument with information on the impacts of changes in GLOBAL:PBRINE and the PCS on brine inflow.		✓		
194.32 SCOPE OF PERFORMANCE ASSESSMENT **2-32-S17.** Please supplement the screening argument with information on the impacts of changes in GLOBAL:PBRINE and the PCS on the availability of brine in the waste panels.		✓		
194.32 SCOPE OF PERFORMANCE ASSESSMENT **2-32-S18.** Please supplement the screening argument with an expanded discussion of the importance of the availability of brine on the degradation of organic material. Changes that affect the availability of brine in a waste panel, such		✓		
194.32 SCOPE OF PERFORMANCE ASSESSMENT **2-32-S19.** Please modify the screening argument to acknowledge the reduced thermal impact of seal concrete hydration because of the elimination of additional explosion walls and the Option D monolith.		✓		
194.32 SCOPE OF PERFORMANCE ASSESSMENT **2-32-S20**. The reported reason for the screening argument update is not consistent between Table SCR-1, where the update is due to new radionuclide inventory, and Section SCR-6.5.1.7.2 where the update is due to new		✓		

Status Report of DOE Responses to EPA Completeness Questions				
Completeness Question	**Included in This Submittal**	**Previously Submitted**	**Pending**	**Withdrawn by the EPA**
194.32 SCOPE OF PERFORMANCE ASSESSMENT **2-32-S21.** Please supplement the screening argument with a discussion of the impact of exothermic reactions in the waste panels.		✓		
194.32 SCOPE OF PERFORMANCE ASSESSMENT **2-32-S22.** Please supplement the screening argument with a discussion of the impact on the PA based on a reduced concrete inventory due to DOE now not using the Option D concrete monoliths in the panel closure system.		✓		
194.32 SCOPE OF PERFORMANCE ASSESSMENT **2-32-S23**. Please update the screening argument to provide a description of the as-emplaced properties of the ROM salt now that *in situ* testing has been completed.		✓		
194.32 SCOPE OF PERFORMANCE ASSESSMENT **2-32-S24**. Please update the screening argument to include the chemical composition of the steel bulkheads that are part of the panel closure design.		✓		
194.32 SCOPE OF PERFORMANCE ASSESSMENT **2-32-S25**. Please supplement the screening argument with information on consolidation specific to the ROM salt in the ROMPCS. Such a discussion can be found in Camphouse et al. (2012, Section 2.0. ERMS 557396).		✓		
194.32 SCOPE OF PERFORMANCE ASSESSMENT **2-32-S26**. The screening decision for this FEP was changed from UP (screened in) to SO-P (screened out – low probability). Please supplement the screening argument with a discussion of the chemical degradation of the		✓		
EPA's Completeness Questions Received June 5, 2015				
CHEMISTRY COMMENTS **3-C-1. Assumed Plutonium Oxidation State.** The Pu oxidation state assumed for Performance Assessment (PA) is important because significantly higher brine solubilities are predicted for Pu(III) than for Pu(IV). In Appendix SOTERM Section 3.6.2, results from		✓		
CHEMISTRY COMMENTS **3-C-2. Boron Species in WIPP Brine.** The Compliance Certification Application (CCA) and CRA-2004 refer to the presence of boric acid [$B(OH)_3$] in WIPP brine. However, the CRA-2009 (Appendix SOTERM, Table SOTERM-2) and CRA-2014 (Appendix		✓		

Status Report of DOE Responses to EPA Completeness Questions				
Completeness Question	**Included in This Submittal**	**Previously Submitted**	**Pending**	**Withdrawn by the EPA**
CHEMISTRY COMMENTS **3-C-3. Adequacy of EQ3/6 Database.** The actinide solubility and aqueous speciation data in the EQ3/6 database DATA0.FM1 was last updated using data available in 2002 (Giambalvo 2003, Nowak 2005). Since 2002, relevant data have been developed in	✓			
CHEMISTRY COMMENTS **3-C-4. Exclusion of Experimental Data with Borate from Am(III) Solubility Uncertainty Analysis.** Brush and Domski (2013) used their Criterion G-9 to select data for the actinide solubility uncertainty analysis; Criterion G-9 specifies that experimental solubility data should be excluded if the solutions contained dissolved	✓			
CHEMISTRY COMMENTS **3-C-5. Am(III) Solubility Uncertainty Distribution.** Brush and Domski (2013) used 172 solubility measurements to determine the Am(III) solubility uncertainty distribution:	✓			
CHEMISTRY COMMENTS **3-C-6. Magnesite Formation from MgO Carbonation.** Clayton (2013, Section 2.7) states that "In the event that CO_2 generation is occurring, but brucite is not available in BRAGFLO simulations, MgO will be converted directly to magnesite." EPA has reviewed the potential for		✓		
CHEMISTRY COMMENTS **3-C-7. Lead Inventory, Gas Generation and Water Balance.** In past WIPP performance assessments, lead corrosion has been assumed to have insignificant effects on gas generation because of the relatively small amount of lead in the packaging and waste inventory (EPA 2010).		✓		
CHEMISTRY COMMENTS **3-C-8. Incorrect Reference to Felmy et al. (1996) and Clark and Tait (1996).** Appendix SOTERM, Section 3.6.1.1 states that "Clark and Tait (Clark and Tait 1996) and Felmy et al. (Felmy et al. 1996) have experimentally observed the reduction of Pu(VI) carbonates by either Fe^0 or Fe^{2+} to Pu(IV).		✓		
CHEMISTRY COMMENTS **3-C-9. Intrinsic Colloid Parameter Values.** The concentration (CONCINT) used for intrinsic plutonium colloids in either the Pu(III) or Pu(IV) oxidation state in the actinide source term model was 1×10^{-9} M in the CCA PAVT, the CRA-2004 PABC and the CRA-2009		✓		
CHEMISTRY COMMENTS **3-C-10. Phase 5 Solubility in DATA0.FM1.** EQ3/6 database version DATA0.FMT.R1 was reviewed and accepted during the EQ3/6 code evaluation (SCA 2011, Appendix A). The database used for the WIPP CRA-2014 EQ3/6 actinide solubility calculations was		✓		

Status Report of DOE Responses to EPA Completeness Questions				
Completeness Question	**Included in This Submittal**	**Previously Submitted**	**Pending**	**Withdrawn by the EPA**
CHEMISTRY COMMENTS **3-C-11. Appendix SOTERM Typographical Errors/Errata.** Section SOTERM-3.6.1.3, Page SOTERM-67, line 3: Section SOTERM-3.5.1.1 and Section SOTERM-3.5.1.2 should be Section SOTERM-3.6.1.1 and Section SOTERM-3.6.1.2		✓		
EPA's Completeness Questions Received July 30, 2015				
CHEMISTRY COMMENTS **4-C-1. Waste Incompatibilities and Gas Generation.** The WIPP Technical Assessment Team investigated the mechanisms and chemical reactions that resulted in the breach of at least one waste drum and release of waste material in the WIPP on February 14, 2014 (SRNL		✓		
CHEMISTRY COMMENTS **4-C-2. Reassessment of Inundated Anoxic Steel Corrosion Rate Data.** **a. Experimental Data Used As Inputs For Parameter CORRMCO2** –The DOE needs to justify the values it has adopted for the parameter CORRMCO2 given the range of existing data. In the CRA-2014 PA the	✓			
CHEMISTRY COMMENTS **4-C-3. Humid Steel Corrosion Rates.** Roselle (2013) states that steel coupons hung in a humid environment exhibited essentially no corrosion regardless of CO_2 concentration. This statement contradicts the experimental data (reported in Roselle, 2013)	✓			
CHEMISTRY COMMENTS **4-C-4. Steel Surface Area per Unit Volume in the Repository.** The anoxic steel gas generation rate due to corrosion is proportional to the steel surface area per unit volume, D_s, (Appendix PA Equation PA.67) in the repository. The parameter D_s is defined by the following equation and		✓		
CHEMISTRY COMMENTS **4-C-5. Steel Sulfidation Rate.** The rate of gas production by sulfidation of iron in steel is determined by the rate of H_2S production through microbial degradation of cellulose and the stoichiometric coefficient for gas generation by sulfidation of steel		✓		
CHEMISTRY COMMENTS **4-C-6. Effects of Green Rust Formation on Gas Generation Stoichiometry.** The stoichiometric coefficient used in PA for gas generation due to steel corrosion (STOIFX) has been maintained at its historical value of 1. This parameter value of "1" assumes no green rust will form on steel. The	✓			
194.14/15 CONTENT OF COMPLIANCE CERTIFICATION APPLICATION/CONTENT OF COMPLIANCE RECERTIFICATION APPLICATION(S). **4-(14)15-1 Plan View of the Repository with Updated Dimensions.** The repository layout has changed since the 2009 recertification. Please provide a plan view of the repository	✓			

Status Report of DOE Responses to EPA Completeness Questions				
Completeness Question	**Included in This Submittal**	**Previously Submitted**	**Pending**	**Withdrawn by the EPA**
194.23 MODELS AND COMPUTER CODES **4-23-1 Volume of Repository Operations and Experimental Areas.** Please clarify the planned excavated volume of the repository operations and experimental areas, accounting for past and current activities and excavations for planned experimental activities in the underground. On		✓		
Addendums as Agreed by the DOE and EPA at the Technical Exchange Meeting Held in Albuquerque, New Mexico, on February 2 and 3, 2016				
Addendum to 1-23-12 WIPP-Specific Organic Complexation Data. Provide thorium(IV) background complexation information.	✓[1]			
Addendum to 2-C-6 MgO Hydration Rate. Explain the status of hydration rate data for Martin Mariette MgO.	✓[1]			
EPA's Completeness Questions Received February 26, 2016				
1. Addendum to Comment 2-C-4 (a) In completeness comment 2-C-4, EPA stated that DOE must re-evaluate the rate of hydromagnesite conversion to magnesite that was used in the CRA 2014 PA (Edwards 2015). DOE's response to this comment (Franco 2015) indicates that there was confusion about the meaning of this comment.	✓[2]			
2-32-S16. Please supplement the screening argument with information on the impacts of changes in GLOBAL:PBRINE and the PCS on brine inflow.				✓[3]
2-32-S17. Please supplement the screening argument with information on the impacts of changes in GLOBAL:PBRINE and the PCS on the availability of brine in the waste panels.				✓[3]

Notes:

[1] Addendum provided based on an agreement made at a DOE/CBFO and EPA technical exchange meeting in Albuquerque, NM on February 2 and 3, 2016.

[2] Addendum provided as requested in the EPA's February 26, 2016 letter.

[3] Completeness questions withdrawn as noted in the EPA's February 26, 2016 letter.

CBFO Management

Briefing Sheet

<table>
<tr><td>Subject:</td><td>Eighth response to the pending EPA completeness letters received to date on the 2014 Compliance Recertification Application (CRA-2014)</td></tr>
<tr><td>Date:</td><td>DOE/CBFO to submit the eighth response to EPA's CRA-2014 completeness questions, June 2016.
Note: June 2016 is a suggested date for DOE's submittal. EPA did not specify a due date for this response submittal.</td></tr>
<tr><td>Summary:</td><td>In response to the EPA CRA-2014 completeness review letters dated June 5, 2015, July 30, 2015, and February 26, 2016, the DOE/CBFO is submitting the eighth set of responses to EPA that consists of:
Enclosure 1 – 7 responses and 3 addendums requested by the EPA.
Enclosure 2 – Electronic copies of the references as noted in each response.
Enclosure 3 – "Status Report of DOE Responses to EPA Completeness Questions." The Table shows the status of responses to the EPA comments received on December 17, 2014, February 27, 2015, June 5, 2015, July 30, 2015 and February 26, 2016.
Enclosure 4 – "CRA-2014 Errata Tracking." The table is a cumulative list of errata that have been identified and corrected up to this point.
With this submittal, the DOE/CBFO is providing responses to all of the remaining EPA completeness questions on the 2014 Compliance Recertification Application received to date.

Status of DOE/CBFO Responses to EPA's CRA-2014 Completeness Questions
<table><tr><th>EPA Letters (Date Issued)</th><th>Total Completeness Questions</th><th>Total Responses Previously Submitted</th><th>Included in this 8th Submittal Package</th></tr><tr><td>12/17/14</td><td>22</td><td>22</td><td>0 Responses</td></tr><tr><td>2/27/15</td><td>40</td><td>40</td><td>2 Addendums</td></tr><tr><td>6/5/15</td><td>11</td><td>8</td><td>3 Responses</td></tr><tr><td>7/30/15</td><td>8</td><td>4</td><td>4 Responses</td></tr><tr><td>2/26/16</td><td>1</td><td>0</td><td>1 Addendum</td></tr></table></td></tr>
<tr><td>Action Requested:</td><td>Review, concur on blue sheet and sign letter.</td></tr>
</table>

CRA-2014 Errata Tracking						
Error #	**Error Description**	**Correction**	**Originator**	**Responsibility**	**Status**	**Date of Completion**
1	EPA Comment 1-23-13 Missing Reference. Appendix SOTERM, Figure SOTERM-7 caption cites Altmaier (2011) but this reference is missing from the reference list. Please provide this reference.	This is a typographical error in Appendix SOTERM. The text will be corrected to read "Altmaier et al., 2008" which is already included as a reference in Appendix SOTERM, given below. The requested reference is included in Enclosure 2. Figure SOTERM-7 is based on Figure 5 in this reference and shows the highest three CaCl2 concentrations shown in the published Figure. This typographical error has been added to Enclosure 4, *CRA-2014 Errata Tracking*. Reference: Altmaier M., Neck, V., Fanghänel, T., "Solubility of Zr(IV), Th(IV) and Pu(IV) hydrous oxides in CaCl2 solutions and the formation of ternary Ca-M-OH complexes," Radiochimica Acta 96, (2008).	EPA	LANL-D. Reed	Included in first response submittal to EPA	Submitted to EPA in first response, 1/28/15
2	EPA Comment 1-G-1 Reference Appendix QAPD-2014 Not Provided. CRA-2014 Section 23, Models and Computer Codes, Section 23.5.7 states, "The DOE's quality assurance program, as applied to the CRA-2014, is contained in Appendix QAPD-2014." The appendix has not been provided. Please provide this document.	There was not an Appendix QAPD-2014 in the CRA-2014; therefore, the statement above is a typographical error in CRA-2014 Section 23.5.7. The reference to Quality Assurance Program Document (QAPD) will be added to Section 23 References and the text will be corrected to read, "The DOE's quality assurance program, as applied to the CRA-2014, is contained in the Quality Assurance Program Document (U.S. DOE 2010)." The QAPD is already included as a reference in the CRA-2014; however, a copy of the QAPD is included in Enclosure 2. This typographical error has been added to Enclosure 4, *CRA-2014 Errata Tracking*.	EPA	SNL-G. Safley	Included in first response submittal to EPA	Submitted to EPA in first response, 1/28/15
3	EPA Comment 2-55-1 Incorrect Reference. IGP-2014, Section IGP-2.1 makes reference to 194.55(b)(1), should this be 194.54(b)(1) "Existing boreholes…"?	This is a typographical error in Appendix IGP-2014. The text will be corrected to read "Existing boreholes, as required by 40 CFR § 194.54(b)(1)…". This typographical error has been added to Enclosure 4, *CRA-2014 Errata Tracking*.	EPA	SNL/JHA- S. Wagner	Included in third response submittal to EPA	Submitted to EPA in third response, 4/8/15

CRA-2014 Errata Tracking						
Error #	**Error Description**	**Correction**	**Originator**	**Responsibility**	**Status**	**Date of Completion**
4	EPA Comment 2-23-2 Provide an Update of the Derivation of the Shaft Properties at the Repository Horizon. "...In the CRA 2014 PA, however, it appears the material properties of the shaft at the repository horizon have not been updated to reflect the change. Please confirm this and identify how the properties would change to reflect the change in the panel closure design."	The corrected length of the northernmost set of panel closures will be implemented in future PA calculations and will be tracked in Enclosure 4, *CRA-2014 Errata Tracking*.	EPA	SNL-T. Zeitler	Included in fourth response submittal to EPA	Submitted to EPA in fourth response, 5/29/15

CRA-2014 Errata Tracking						
Error #	**Error Description**	**Correction**	**Originator**	**Responsibility**	**Status**	**Date of Completion**
5	EPA Comment 2-32-S7 FEP W3 Heterogeneity of Waste Forms. The screening argument citation of the CCA as the source of information on the heterogeneity of waste forms ignores changes that have occurred in the past 15 years, including supercompacted waste and mingling RH waste in shielded containers with CH waste. Please update the information to reflect current waste forms.	SCR-6.1.2.1.2 Summary of New Information The waste inventory used for the CRA-2014 PA calculations has been updated as provided in Kicker and Zeitler (2013). Since these FEPs are accounted for in PA, inventory-related parameters may differ from those used in previous PAs; however, the screening decisions have not changed and these FEPs are represented in PA calculations. The EPA approved the use of the shielded RH container as an allowable disposal container in WIPP (Edwards 2013). The impacts of this container upon WIPP performance were evaluated in Dunagan et al. (2007). SCR-6.1.2.1.3 Screening Argument Waste characteristics, comprising the waste inventory and heterogeneity of waste forms, are described in the CCA, Appendix BIR. The waste inventory is accounted for in PA calculations in deriving the dissolved actinide source term and gas generation rates. The distribution of contact-handled transuranic (CH-TRU) and remote-handled transuranic (RH-TRU) waste within the repository leads to room-scale heterogeneity of the waste forms, which is accounted for in PA calculations when considering the potential activity of waste material encountered during inadvertent borehole intrusion (Appendix PA-2014, Section PA-3.8). The DOE implements waste heterogeneity in waste forms through the assumption of random placement of TRU waste in the repository. This assumption includes all waste container forms and types. Details regarding the implementation of this assumption are provided in the CRA-2009, Appendix MASS-2009, Section MASS-21.0. This implementation methodology has not changed as a result of the addition of the shielded RH-waste container. This change has been added to Enclosure 4, *CRA-2014 Errata Tracking*.	EPA	SNL/PIRU- R. Kirkes	Included in fourth response submittal to EPA	Submitted to EPA in fourth response, 5/29/15

CRA-2014 Errata Tracking						
Error #	**Error Description**	**Correction**	**Originator**	**Responsibility**	**Status**	**Date of Completion**
6	EPA Comment 2-32-S8 FEP W5 Container Material Inventory. Please supplement the screening argument with an explanation of the implementation in PA of the material inventory of shielded containers containing RH waste.	SCR-6.1.3.2 FEP Number: W5 FEP Title: Container Material Inventory SCR-6.1.3.2.1 Screening Decision: UP The Container Material Inventory is accounted for in PA calculations. SCR-6.1.3.2.2 Summary of New Information The masses of container materials associated with the waste inventory for the CRA-2014 have been updated as detailed in Van Soest (2012). The EPA approved the use of the shielded RH container as an allowable disposal container in WIPP (Edwards 2013). The impacts of this container upon WIPP performance were evaluated in Dunagan et al. (2007). SCR-6.1.3.2.3 Screening Argument The container material inventory is described in Van Soest (2012) and is accounted for in PA calculations through the estimation of gas generation rates (see Appendix PA-2014, Section PA-4.2.5). In the CCA, Appendix WCL, a minimum quantity of metallic Fe was specified to ensure sufficient reactants to reduce radionuclides to lower and less soluble oxidation states. This requirement is met as long as there are no substantial changes in container materials. The inventory used for the CRA-2014 contains 3.69 x 107 kg of steel in packaging (includes containers) materials. This value is up slightly from 3.59 x 107 kg reported in 2008 (Van Soest 2012). Modeling assumptions related to the implementation of waste container materials can be found in Appendix MASS-2014, Table MASS-5. This change has been added to Enclosure 4, *CRA-2014 Errata Tracking*.	EPA	SNL/PIRU- R. Kirkes	Included in fourth response submittal to EPA	Submitted to EPA in fourth response, 5/29/15

CRA-2014 Errata Tracking						
Error #	**Error Description**	**Correction**	**Originator**	**Responsibility**	**Status**	**Date of Completion**
7	EPA Comment 2-32-S15 FEP W28 Nuclear Explosions. Please modify the screening argument to address whether, in addition to "a reduction of TRU radionuclides from previous estimates", the quantities of fissile radionuclides have also been reduced.	SCR-6.3.3.2 FEP Number: W28 FEP Title: Nuclear Explosions SCR-6.3.3.2.1 Screening Decision: SO-P Nuclear Explosions have been eliminated from PA calculations on the basis of low probability of occurrence over 10,000 yrs. SCR-6.3.3.2.2 Summary of New Information This FEP has been updated to include the most recent inventory information as presented in Kicker and Zeitler (2013). This new information does not change the screening argument or decision for this FEP. SCR-6.3.3.2.3 Screening Argument Nuclear explosions have been eliminated from PA calculations on the basis of low probability of occurrence over 10,000 yrs. For a nuclear explosion to occur, a critical mass of Pu would have to undergo rapid compression to a high density. Even if a critical mass of Pu could form in the system, there is no mechanism for rapid compression. Inventory information used for the CRA-2014 is presented in Kicker and Zeitler (2013). The updated inventory information for the CRA-2014 shows a reduction of TRU radionuclides from previous estimates. Fissile radionuclides have reduced from approximately 3.1 million curies for the PABC-2009 to 2.7 million curies for the CRA-2014. Thus, current criticality screening arguments are conservatively bounded by the previous CCA screening arguments (Rechard et al. 1996, 2000, and 2001). This change has been added to Enclosure 4, *CRA-2014 Errata Tracking*.	EPA	SNL/PIRU- R. Kirkes	Included in fourth response submittal to EPA	Submitted to EPA in fourth response, 5/29/15

CRA-2014 Errata Tracking						
Error #	**Error Description**	**Correction**	**Originator**	**Responsibility**	**Status**	**Date of Completion**
8	EPA Comment 2-32-S19 FEP W45 Effects of Temperature on Microbial Gas Generation. Please modify the screening argument to acknowledge the reduced thermal impact of seal concrete hydration because of the elimination of additional explosion walls and the Option D monolith.	This is a revision to Appendix SCR-2014, Section SCR-6.5.1.1.3.1. The revised text has been changed to read: This thermal rise is considered bounding due to the elimination of concrete from the panel closure systems. Because the new panel closures will be constructed of mined salt, the overall mass of concrete emplaced within the repository will be significantly decreased. More importantly, the emplacement of any constructed element (e.g., shaft seals) of the repository will be done at or before repository closure. Therefore, any increase in temperature due to concrete hydration will have abated by the time AICs are assumed to no longer prevent drilling into the repository. The revised text has been added to Enclosure 4, *CRA-2014 Errata Tracking*.	EPA	SNL/PIRU- R. Kirkes	Included in fourth response submittal to EPA	Submitted to EPA in fourth response, 5/29/15
9	EPA Comment 2-32-S20 FEP W53 Radiolysis of Cellulose. The reported reason for the screening argument update is not consistent between Table SCR-1, where the update is due to new radionuclide inventory, and Section SCR-6.5.1.7.2 where the update is due to new cellulose inventory. The screening argument in Section SCR-6.5.1.7.3 refers only to the new radionuclide inventory. Please reconcile the information.	This is a revision to Appendix SCR-2014. The revised text of Section SCR-6.5.1.7.2 has been changed to read: SCR-6.5.1.7.2 Summary of New Information This FEP has been updated with new waste inventory data. Decreasing waste inventory values lower the overall activity for all TRU radionuclides which indicate that radiolysis of cellulose will not be a significant process. The screening argument and decision are not affected by this change in inventory information. This change has been added to Enclosure 4, *CRA-2014 Errata Tracking*.	EPA	SNL/PIRU- R. Kirkes	Included in fourth response submittal to EPA	Submitted to EPA in fourth response, 5/29/15

CRA-2014 Errata Tracking						
Error #	**Error Description**	**Correction**	**Originator**	**Responsibility**	**Status**	**Date of Completion**
10	EPA Comment 2-32-S1 FEP H21 Drilling Fluid Flow. Screening argument considers only boreholes intersecting the waste region. Please supplement the argument with a discussion of boreholes that intersect the non-waste regions and the consequence to PA calculations. Provide references and specific information as to whether boreholes penetrating non-waste regions could result in the transport of radionuclides between the waste and non-waste regions, to overlying units, or to the surface. Provide information, either directly or by reference, as to how deep boreholes penetrating the non-waste and waste regions of the repository are accounted for in the PA.	This is a revision to Appendix SCR-2014, Section SCR-5.2.1.1. The revised text that has been changed to address EPA Comment 2-32-S1 is documented in blue font type in Enclosure 1 of DOE's fifth response submittal to EPA.	EPA	SNL/PIRU- R. Kirkes	Included in fifth response submittal to EPA	Submitted to EPA in fifth response, 7/15/15
11	EPA Comment 2-32-S2 FEP H22 Drilling Fluid Loss. The screening argument considers flow into the repository from boreholes that intercept pressurized fluid in underlying formations but only for boreholes intersecting the waste region. In the current BRAGLO model gas and brine readily flow between the waste and non-waste regions. A discussion and analysis of boreholes that could intersect the non-waste regions and their impact on the PA needs to be provided.	This is a revision to Appendix SCR-2014, Section SCR-5.2.1.2. The revised text that has been changed to address EPA Comment 2-32-S2 is documented in blue font type in Enclosure 1 of DOE's fifth response submittal to EPA.	EPA	SNL/PIRU- R. Kirkes	Included in fifth response submittal to EPA	Submitted to EPA in fifth response, 7/15/15

CRA-2014 Errata Tracking						
Error #	**Error Description**	**Correction**	**Originator**	**Responsibility**	**Status**	**Date of Completion**
12	EPA Comment 2-32-S3 FEP H23 Blowouts. Screening argument considers only boreholes intersecting the waste region and also pressurized Castile brine. In the current BRAGLO model gas and brine readily flow between the waste and non-waste regions. Please supplement the argument with a discussion and analysis of boreholes that could intersect the non-waste regions on the PA.	This is a revision to Appendix SCR-2014, Section SCR-5.2.1.3. The revised text that has been changed to address EPA Comment 2-32-S3 is documented in blue font type in Enclosure 1 of DOE's fifth response submittal to EPA.	EPA	SNL/PIRU- R. Kirkes	Included in fifth response submittal to EPA	Submitted to EPA in fifth response, 7/15/15
13	EPA Comment 2-32-S11 FEP W20 Salt Creep. Please supplement the screening argument with a discussion of salt creep and consolidation to the ROM salt in the ROMPCS, and healing of the adjacent DRZ. Such a discussion can be found in Camphouse et al. (2012, Section 2.0. ERMS 557396). The screening argument for this FEP states that "Salt creep in the Salado is accounted for in PA calculations (the CCA, Chapter 6.0, Section 6.4.3.1)." The cited CCA section discusses these FEPs only in the context of the waste region. In addition, this is the only FEP that addresses DRZ healing, which is expected to vary spatially.	This is a revision to Appendix SCR-2014, Section SCR-6.3.1.2. The revised text that has been changed to address EPA Comment 2-32-S11 is documented in blue font type in Enclosure 1 of DOE's fifth response submittal to EPA.	EPA	SNL/PIRU- R. Kirkes	Included in fifth response submittal to EPA	Submitted to EPA in fifth response, 7/15/15

CRA-2014 Errata Tracking						
Error #	**Error Description**	**Correction**	**Originator**	**Responsibility**	**Status**	**Date of Completion**
14	EPA Comment 2-32-S12 FEP W21 Changes in the Stress. Screening argument was combined with that for W20 Salt Creep; please see comments for FEP W20. Additionally, please supplement the screening argument with discussions of 1) the coupling between consolidation of the ROM salt in the ROMPCS and healing of the adjacent DRZ (DRZ healing cannot occur until the ROM salt is consolidated and applies a back stress sufficient to compress and heal the DRZ); and 2) lateral extrusion of the ROM salt when under compressive stress from drift creep closure.	This is a revision to Appendix SCR-2014, Section SCR-6.3.1.2. The revised text that has been changed to address EPA Comment 2-32-S12 is documented in blue font type in Enclosure 1 of DOE's fifth response submittal to EPA.	EPA	SNL/PIRU- R. Kirkes	Included in fifth response submittal to EPA	Submitted to EPA in fifth response, 7/15/15
15	EPA Comment 2-32-S21 FEP W72 Exothermic Reactions. Please supplement the screening argument with a discussion of the impact of exothermic reactions in the waste panels.	This is a revision to Appendix SCR-2014, Section SCR-6.3.4.1. The revised text that has been changed to address EPA Comment 2-32-S21 is documented in blue font type in Enclosure 1 of DOE's fifth response submittal to EPA.	EPA	SNL/PIRU- R. Kirkes	Included in fifth response submittal to EPA	Submitted to EPA in fifth response, 7/15/15

CRA-2014 Errata Tracking						
Error #	**Error Description**	**Correction**	**Originator**	**Responsibility**	**Status**	**Date of Completion**
16	EPA Comment 3-C-11. Appendix SOTERM Typographical Errors/Errata. Section SOTERM-3.6.1.3, Page SOTERM-67, line 3: Section SOTERM-3.5.1.1 and Section SOTERM-3.5.1.2 should be Section SOTERM-3.6.1.1 and Section SOTERM-3.6.1.2 Appendix SOTERM, Section SOTERM-6.0 References: The correct date for the following reference is 2010: Reed, D.T., J.-F. Lucchini, M. Borkowski, and M.K. Richmann. 20092010. Reduction of Higher Valent Plutonium by Iron under Waste Isolation Pilot Plant (WIPP) - Relevant Conditions: Data Summary and Recommendations. LCO-ACP-09, LANL\ACRSP Report. Los Alamos, NM: Los Alamos National Laboratory.	These are typographical errors in Appendix SOTERM-2014. The cross-references in Section 3.6.1.3 should be SOTERM-3.6.1.1 and SOTERM-3.6.1.2, as the EPA has noted. This sentence in Appendix SOTERM-2014 is changed to read: The overall issue of a thermodynamic driver for higher-valent Pu oxides, although it has received much recent attention in the literature, is not yet resolved, but has a relatively insignificant impact on the WIPP regardless of the mechanisms at work. A prolonged unsaturated phase in the WIPP could lead to the formation of some PuO2+x, but this will be quickly overwhelmed in an aqueous environment and the higher-valent Pu will be reduced to Pu(III/IV) species, as described in Section SOTERM-3.6.1.1 and Section SOTERM-3.6.1.2. Both DBR and transport-release scenarios assume brine inundation and, correspondingly, the rapid introduction of reducing conditions. Although the plutonium internal report is labeled as a 2009 report, it was finalized in 2010 – so DOE agrees with the EPA that 2010 is the correct date of reference for the report. The reference for this report is changed to the following: "Reed, D.T., J.-F. Lucchini, M. Borkowski, and M.K. Richmann. 2010. Reduction of Higher Valent Plutonium by Iron under Waste Isolation Pilot Plant (WIPP) - Relevant Conditions: Data Summary and Recommendations. LCO-ACP-09, LANL\ACRSP Report. Los Alamos National Laboratory, Los Alamos, NM." A copy of this reference is provided in Enclosure 2. Also, "Reed et al. 2009" is replaced with "Reed et al. 2010" in the following locations: SOTERM vi Figure SOTERM-15 caption SOTERM 18 Line 8 SOTERM 36 Line 27 SOTERM 62 Line 14 SOTERM 65 Line 4 (Figure 15 caption) These typographical errors have been added to Enclosure 4, *CRA-2014 Errata Tracking*.	EPA	LANL-D. Reed	Included in fifth response submittal to EPA	Submitted to EPA in fifth response, 7/15/15

CRA-2014 Errata Tracking						
Error #	**Error Description**	**Correction**	**Originator**	**Responsibility**	**Status**	**Date of Completion**
17	EPA Comment 3-C-8. Incorrect Reference to Felmy et al. (1996) and Clark and Tait (1996). Appendix SOTERM, Section 3.6.1.1 states that "Clark and Tait (Clark and Tait 1996) and Felmy et al. (Felmy et al. 1996) have experimentally observed the reduction of Pu(VI) carbonates by either Fe^0 or Fe^{2+} to Pu(IV). However, the Felmy et al. citation refers to a study of thorium(IV) hydrous oxide solubility and Clark and Tait (1996) indicate that plutonium(VI) chloride complexes were reduced to plutonium(V) by Fe^0 or Fe^{2+}. Please provide the correct references. Clark, D.L., and C.D. Tait. 1996. Memorandum to Sandia WIPP Records Center (Subject:SWCF-A: 1.1.10.1.1: NQ: Actinide Source Term: LANL Monthly Reports). Sandia National Laboratories, WIPP Central File A: WBS 1.1.10.1.1. WPO 31106. Felmy, A.R., D. Rai, S.M. Sterner, M.J. Mason and N.J. Hess. 1996. Thermodynamic models for highly charged aqueous species: solubility of Th(IV) hydrous oxide in concentrated $NaHCL_3$ and Na_2CO_3 solutions. Sandia National Laboratories, ERMS 240226.	To address this issue, Section 3.6.11 of Appendix SOTERM-2014, has been revised as follows (provided in blue font below): From Appendix SOTERM-2014, Section 3.6.1.1 In geochemical systems, redox control is often interpreted in terms of the iron, and in a broader sense, reduced metal, mineralogy, and associated aqueous chemistry (Sanchez, Murray, and Sibley 1985; White, Yee, and Flexser 1985). In the WIPP case, iron will undergo anoxic corrosion, producing Fe^{2+}. Both metallic iron (Fe^0) and Fe^{2+} have been shown to quantitatively reduce Pu(VI) in the WIPP brines to either Pu(IV) or Pu(III)(Reed et al. 2006; Reed et al. 2009). ~~Clark and Tait (1996) and Felmy et al. (1996) have experimentally observed the reduction of Pu(VI) carbonates by either Fe0 or Fe2+ to Pu(IV). In the absence of carbonates, a quantitative reduction of Pu(VI) is also observed, but the oxidation state of the resulting species cannot be definitively determined because its concentration is below the lower detection limit of the oxidation state analytical process (about 10-9 M). However, since this concentration is well below the expected solubility of Pu(V) species, it was reasonably assumed that the Pu must have been reduced to either the IV or III oxidation state.~~ Neretnieks (1982) has shown that when dissolved actinides in moving groundwater came in contact with Fe(II), the actinides were reduced to a much-less-soluble oxidation state and precipitated. These changes have been added to Enclosure 4, *CRA-2014 Errata Tracking*.	EPA	LANL-D. Reed	Included in seventh response submittal to EPA	Submitted to EPA in seventh response, 12/8/15

CRA-2014 Errata Tracking						
Error #	**Error Description**	**Correction**	**Originator**	**Responsibility**	**Status**	**Date of Completion**
18	EPA Comment 4-C-6. Effects of Green Rust Formation on Gas Generation Stoichiometry. The stoichiometric coefficient used in PA for gas generation due to steel corrosion (STOIFX) has been maintained at its historical value of 1. This parameter value of "1" assumes no green rust will form on steel. The assumption is contradicted in Appendix SOTERM Section 2.3.4 of the CRA-2014, which includes the following statement: Roselle (Roselle 2013) states that green rust is the most likely corrosion product in experiments with low atmospheric CO_2 concentrations (< 350 ppm).	To address this issue, Section 2.3.4 of Appendix SOTERM-2014 incorrectly refers to Roselle's work and has therefore been revised as follows (provided in blue font): "In fact, Roselle (Roselle 2013) states that ~~green rust~~ $Fe(OH)_2$ is the most likely corrosion product in experiments with low atmospheric CO_2 concentrations ~~(<350 ppm)~~." These changes have been added to Enclosure 4, *CRA-2014 Errata Tracking*.	EPA	SNL-Y. Xiong	Included in eighth response submittal to EPA	Submitted to EPA in eighth response
End of CRA-2014 Errata Tracking						